SAND2022-6984C

Sandia National Laboratories

A hybrid mesh-based/element-free approach for analysis on geometrically complex domains without defeaturing

Joe Bishop

Engineering Sciences Center
Sandia National Laboratories
Albuquerque, NM

SAND2022-???? C

U.S. DEPARTMENT OF ENERGY   NNSA

US Congress on Theoretical and Applied Mechanics
June 19-24, 2022, Austin, TX

Sandia National Laboratories is a multimission laboratory managed and operated by National Technology & Engineering Solutions of Sandia, LLC, a wholly owned subsidiary of Honeywell International Inc., for the U.S. Department of Energy's National Nuclear Security Administration under contract DE-NA0003525.

Sandia National Laboratories is a multimission laboratory managed and operated by National Technology & Engineering Solutions of Sandia, LLC, a wholly owned subsidiary of Honeywell International Inc., for the U.S. Department of Energy's National Nuclear Security Administration under contract DE-NA0003525.

Outline

1. motivation
2. hybrid mesh/element-free discretizations
3. weight functions using manifold geodesics
4. quadrature via secondary basis functions
5. strain projections for polynomial consistency
6. verification example, linear elasticity
7. summary

Motivation: Agile simulation of complex assemblies

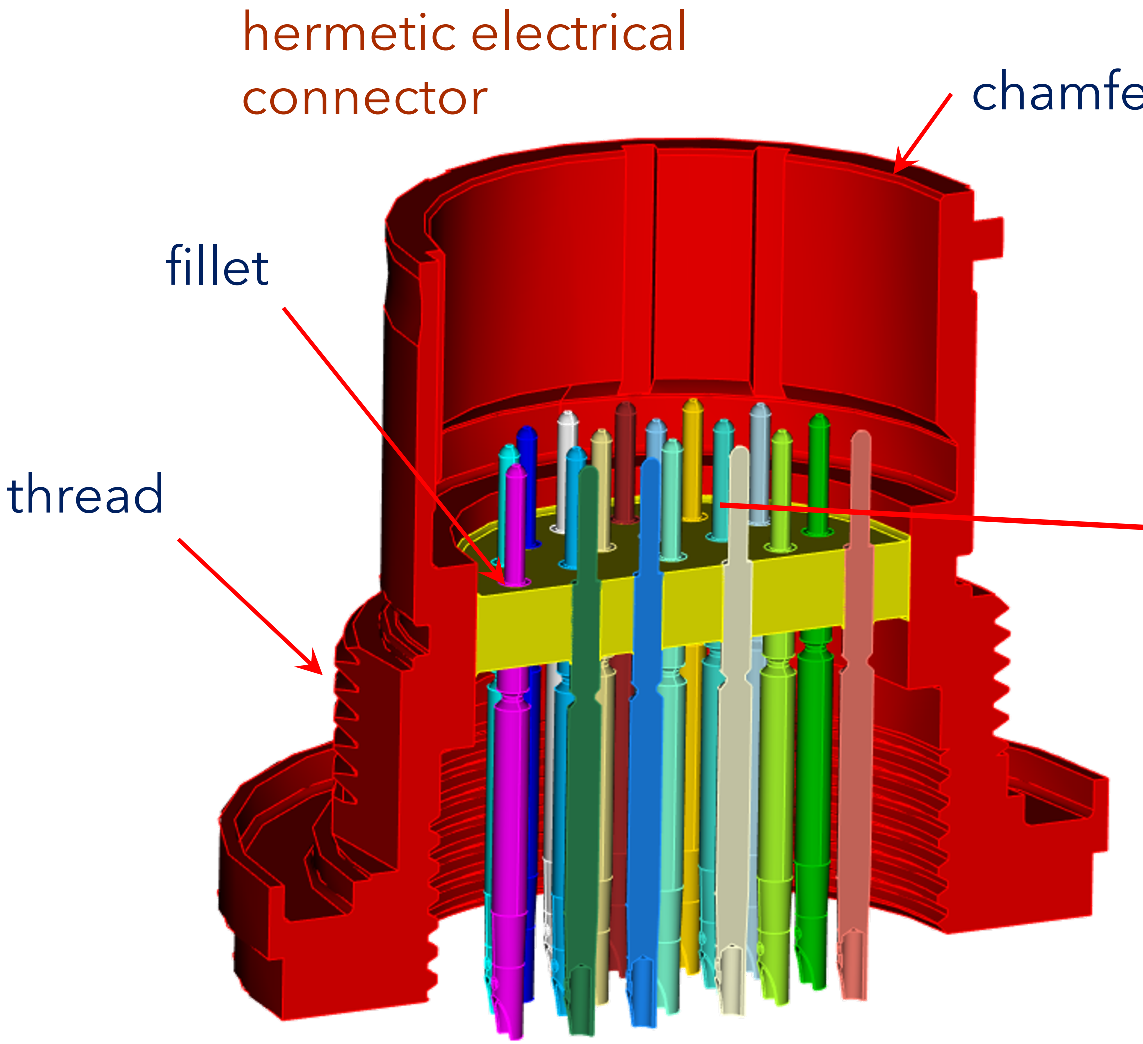

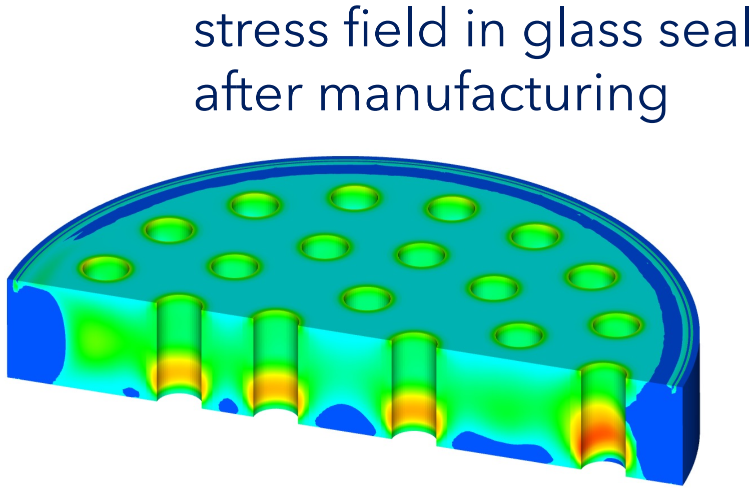

- Domains typically contain many geometric features that must be removed before analysis.
- Heuristics are often used to defeature geometry.
- Heuristics are used to construct finite element mesh.
- Goals of simulation can vary during design process.

Motivation: Image-based analysis

Johnson, et al., 2019, "Predicting the reliability of an additively-manufactured metal part for the third Sandia fracture challenge by accounting for random material defects," *International Journal of Fracture*, v. 218, pp. 231-243

strain field

cut-away view

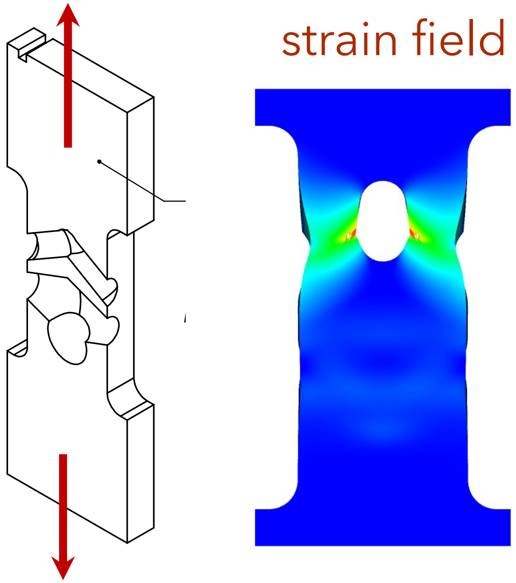

CT reconstruction of AM part (triangulation)

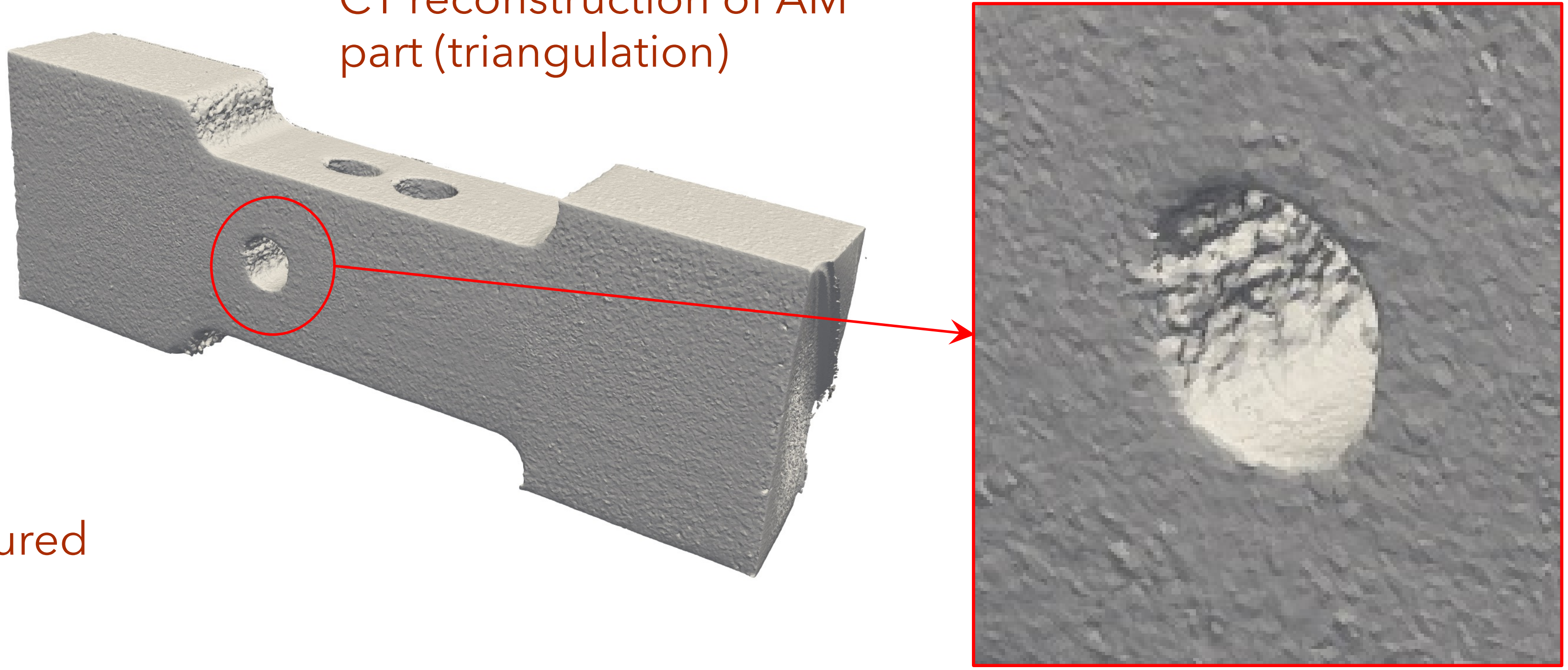

additively manufactured

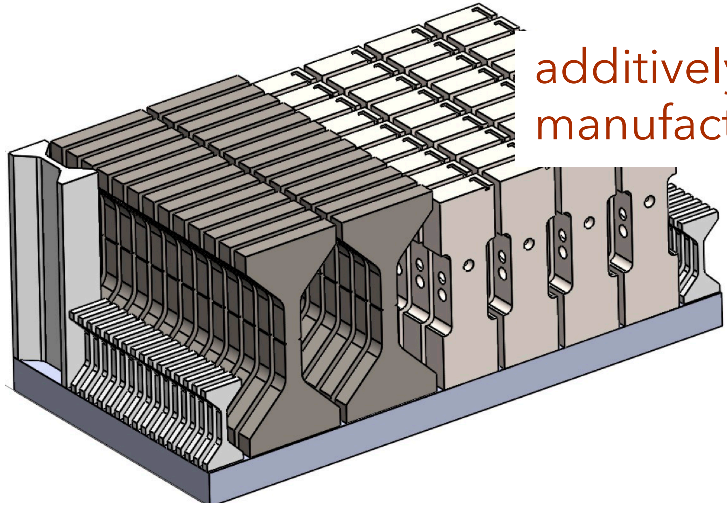

Typical geometric reconstructions require a smoothing or decimation process before modeling can commence.

Motivation: Typical domain (geometry) features

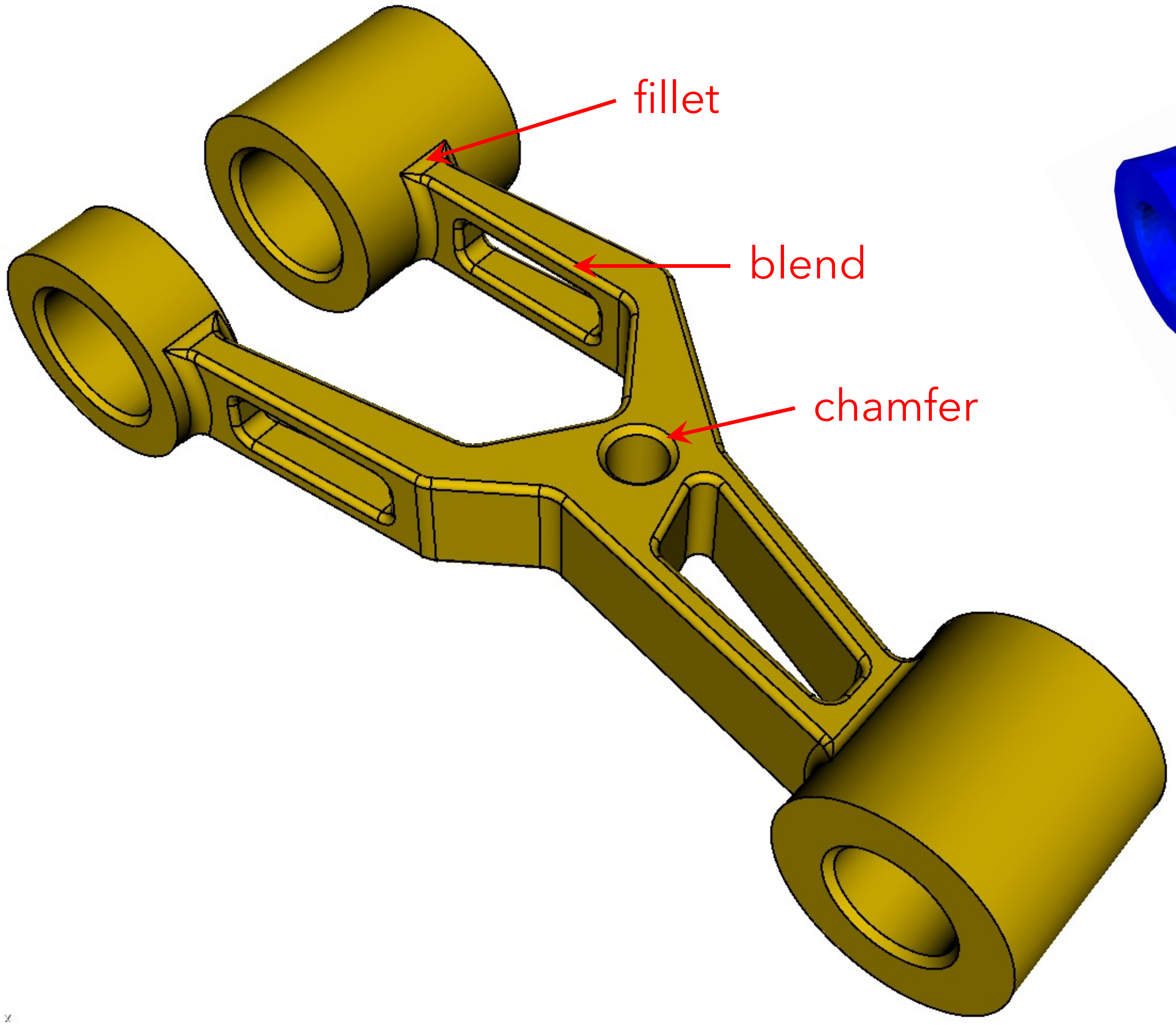

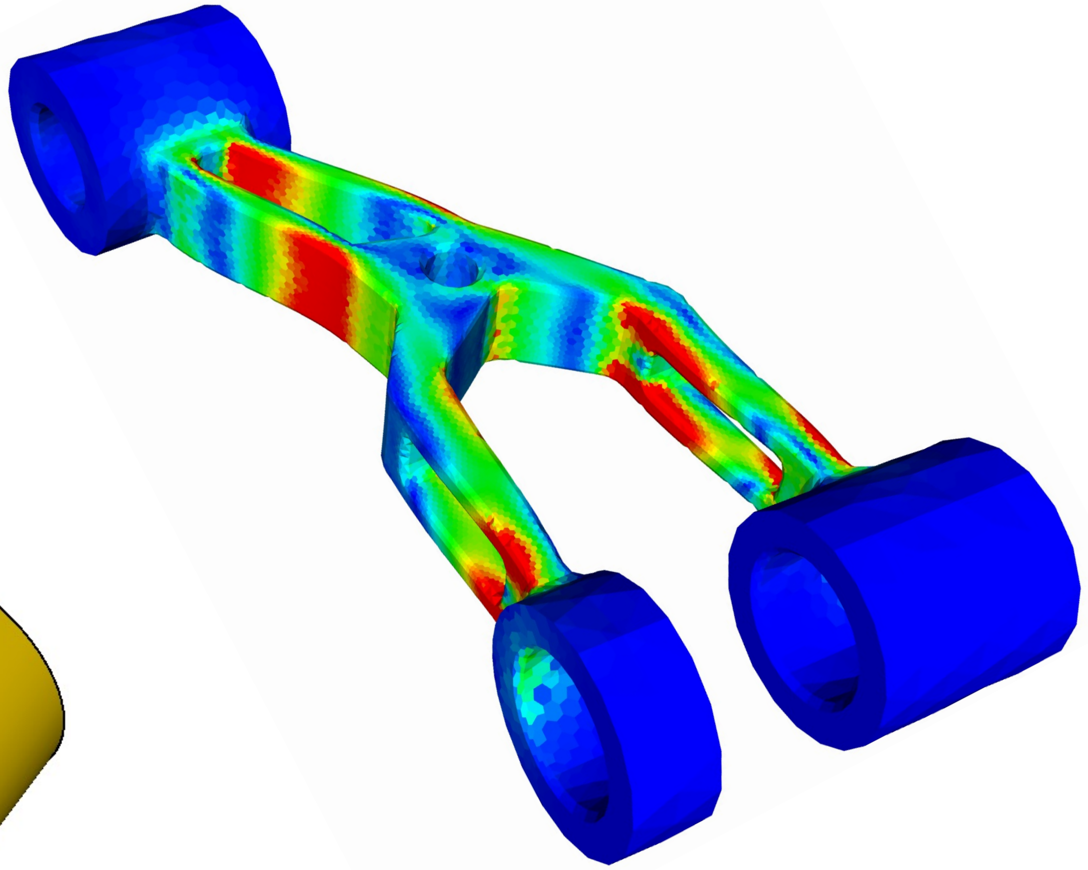

Motivation: Domain discretization

FEA discretization is intimately tied to domain geometry.

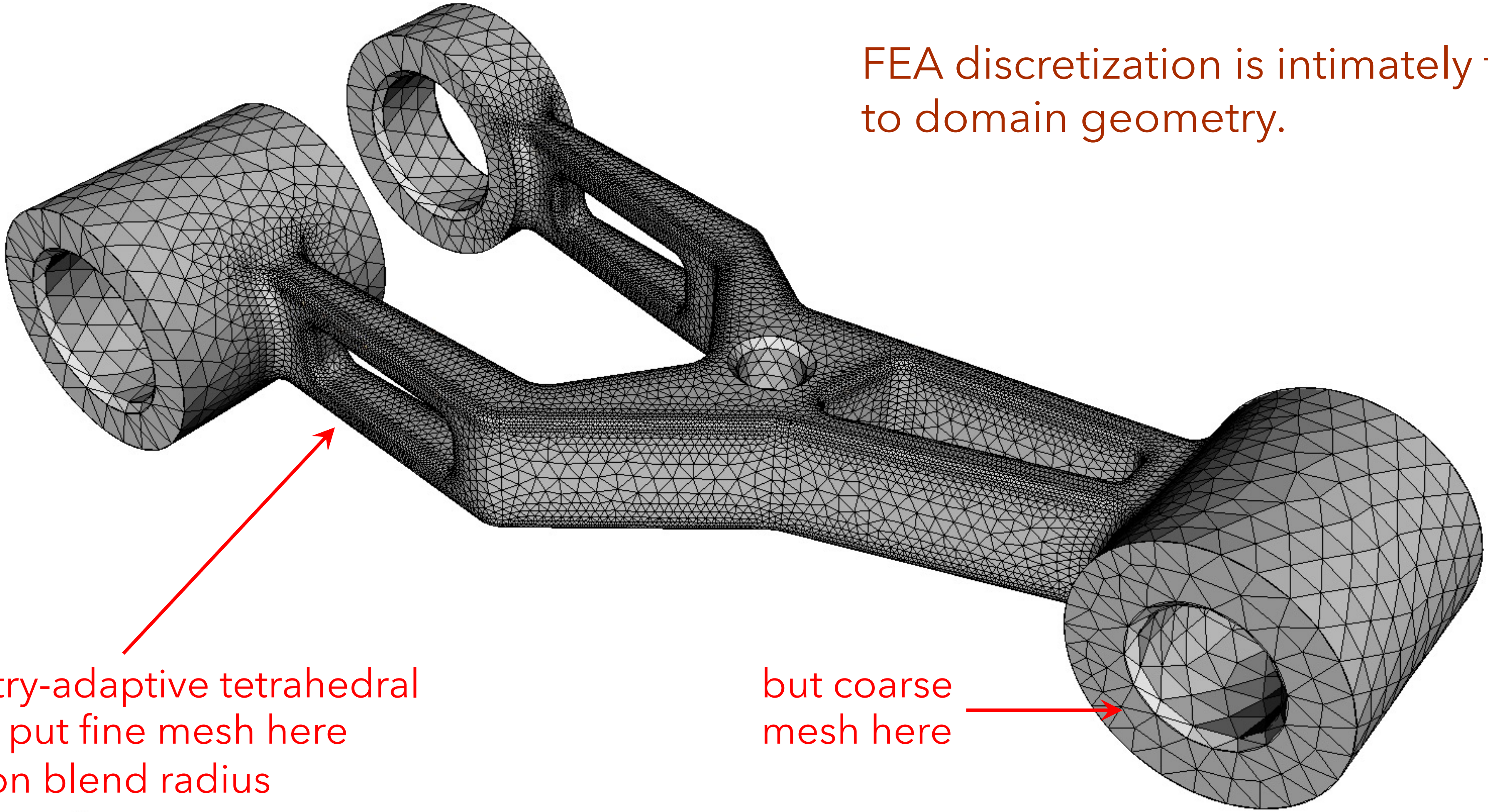

geometry-adaptive tetrahedral mesher put fine mesh here based on blend radius

but coarse mesh here

Motivation: Separate domain discretization from solution discretization

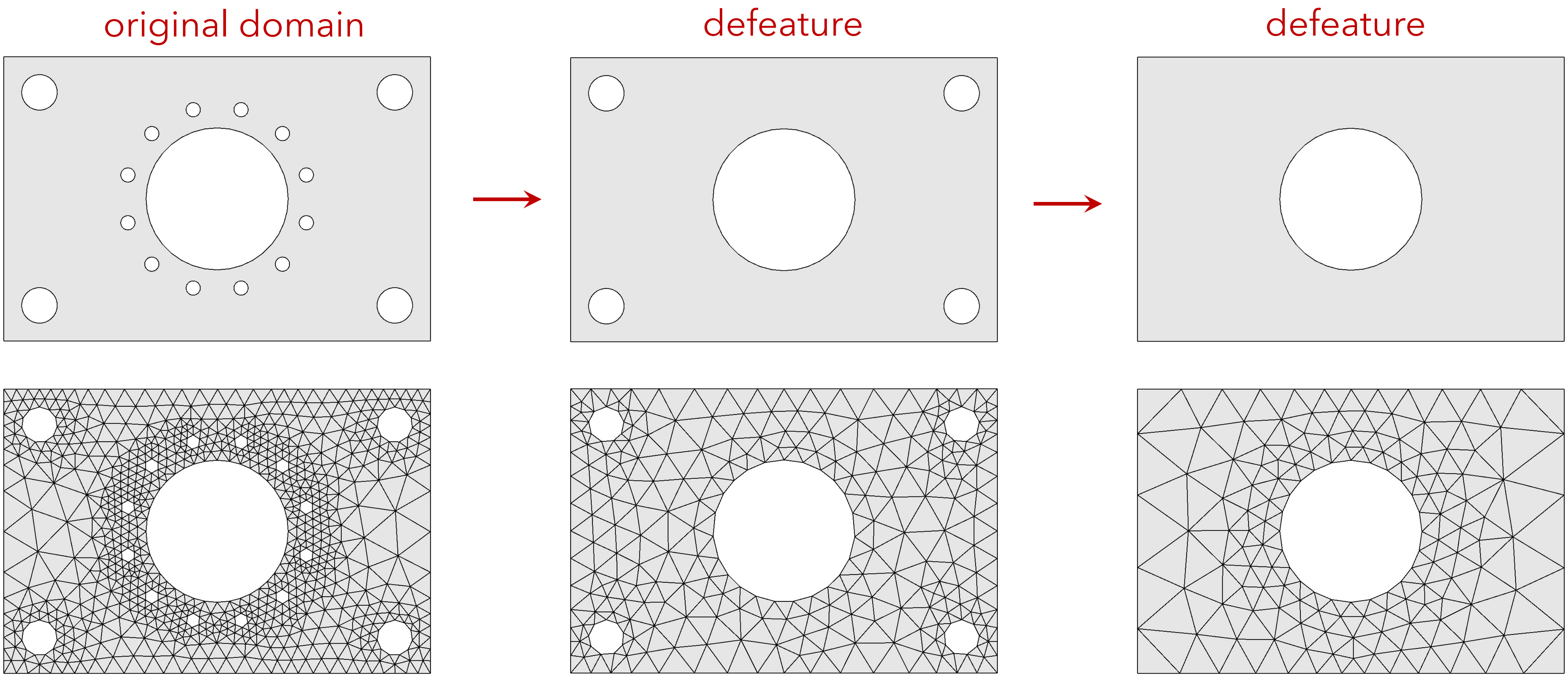

Impact of domain defeaturing? depends on goals of simulation

Motivation: Separate domain discretization from solution discretization

- Domain defeaturing is needed to control FEA discretization quality, size, and critical time step (explicit dynamics)
- Domain defeaturing typically requires human intervention (heuristics).
- For FEA, domain discretization and solution discretization are synonymous (isoparametric).
- Geometric features can require a fine local discretization while solution does not.
- Heuristics are often used in mesh design.
- Meshes are typically designed with goal in mind, thus making it cumbersome to reuse.
- Adaptivity requires going back to geometric model of domain.

Alternative hybrid approach: separate domain discretization and solution approximation using an element-free formulation.

A hybrid element-free approach

finite-element approach

- defeature domain geometry based on goals
- create a mesh based on goals
- mesh discretizes domain and solution
- quadrature of weak form is easy
- visualization of results using mesh
- adaptivity of mesh is hard

mesh-free approach

- no defeaturing of domain geometry
- no discretization of domain
- connectivity of domain is undefined (need computational geometry)
- quadrature of weak form is very hard
- visualization of results is cumbersome

Alternative hybrid approach: separate domain discretization and solution approximation using an element-free formulation.

Hybrid approach: fine-scale triangulation

original domain

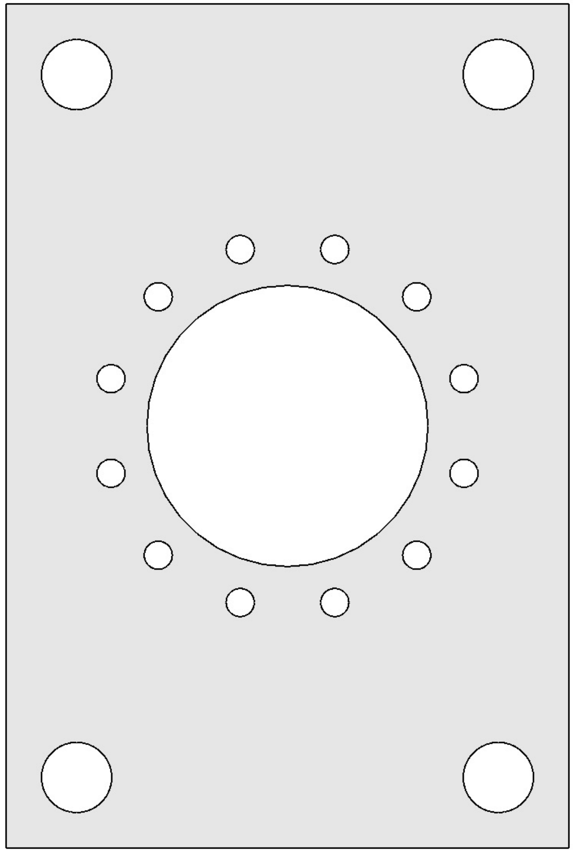

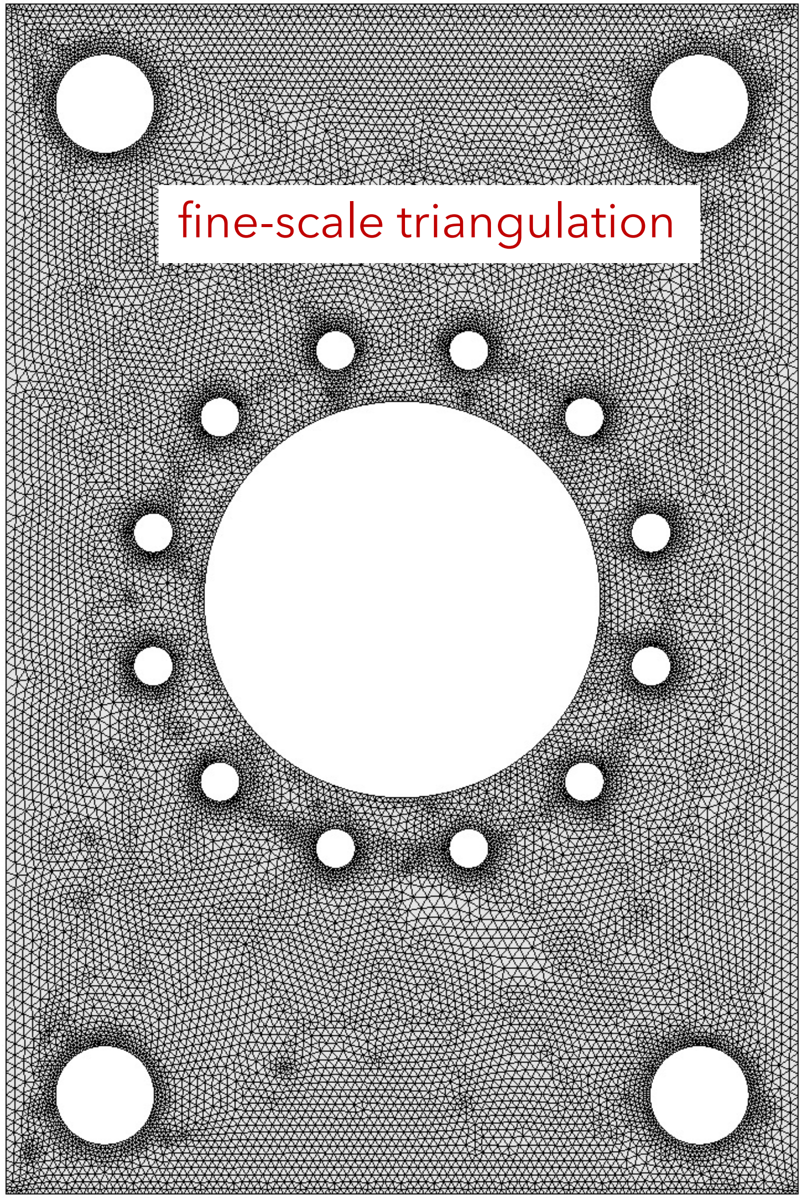

create an element-free basis using triangulation.

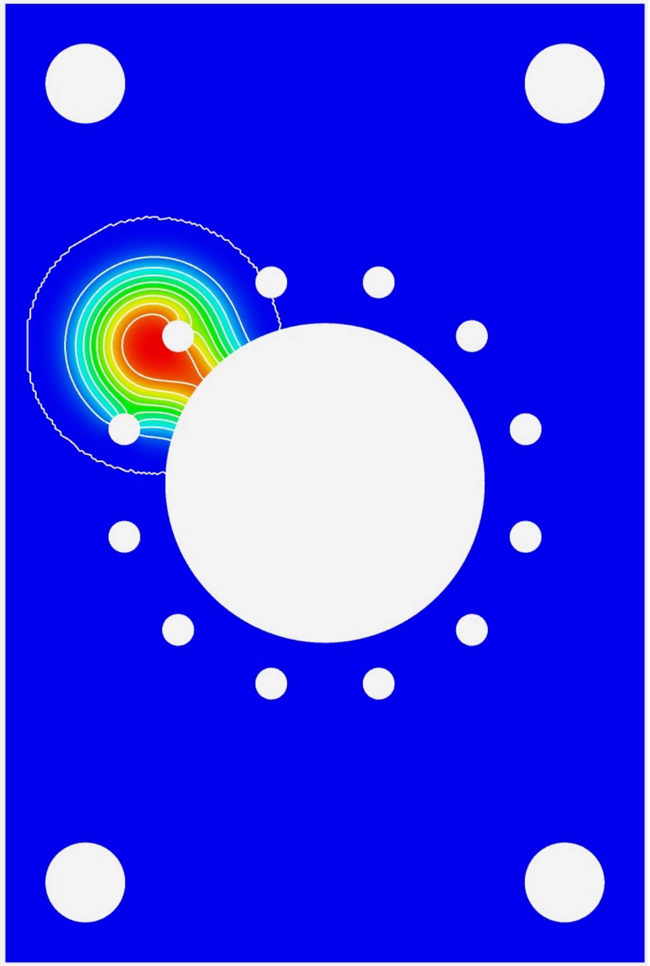

Element-free basis functions

- Element-free basis functions automatically include geometric features at all scales.
- Solution discretization is separate from domain discretization.
- No need to defeature domain.

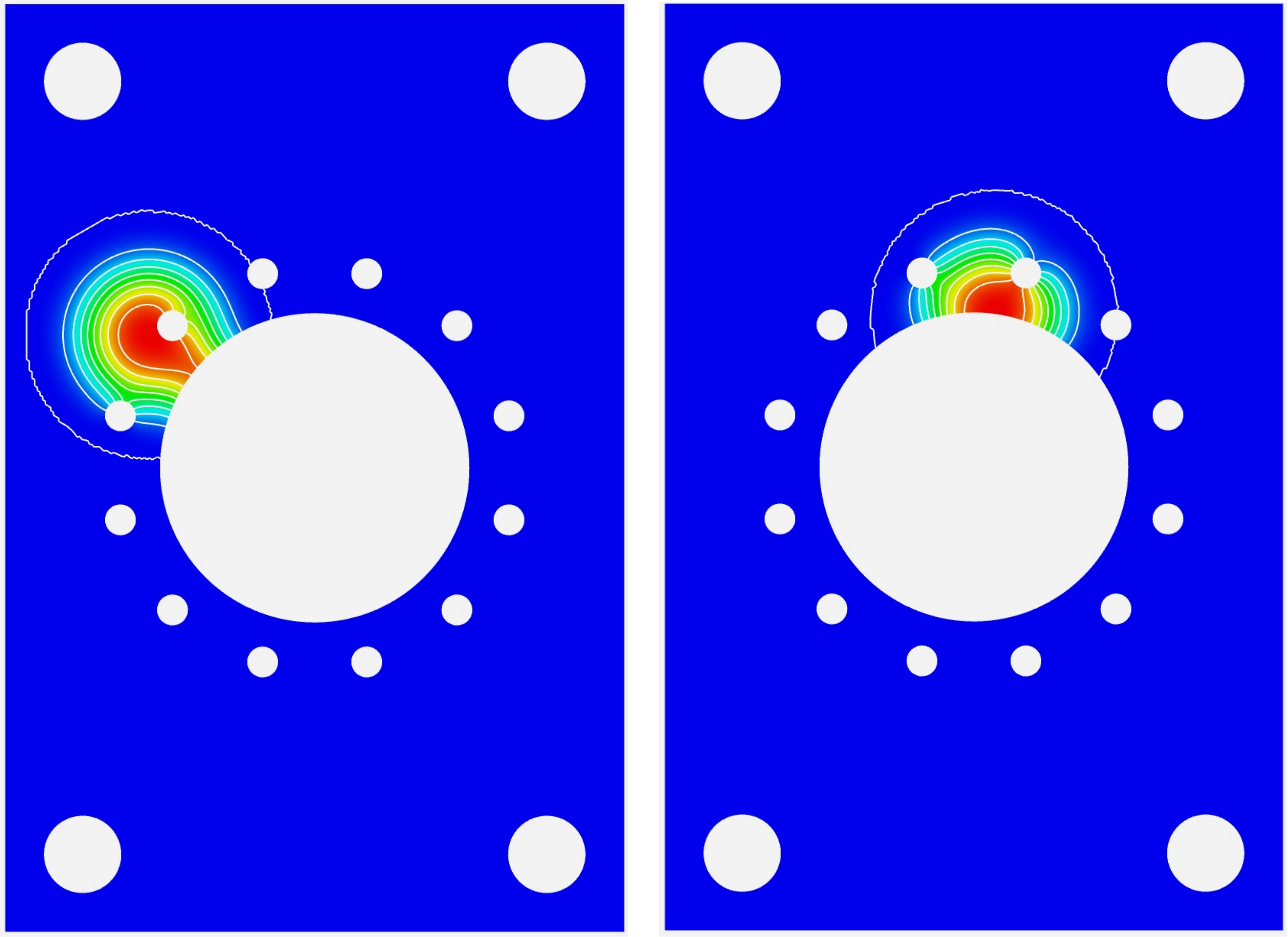

Hybrid approach: fine-scale triangulation

Tet-meshing methods

- Delaunay
- advancing front
- background grid
- envelope

Fast Tetrahedral Meshing in the Wild

ACM Trans. Graph. 2020
vol. 39 Issue 4 Article 117

YIXIN HU, New York University, USA
TESEO SCHNEIDER, New York University, USA
BOLUN WANG, Beihang University, China and New York University, USA
DENIS ZORIN, New York University, USA
DANIELE PANOZZO, New York University, USA

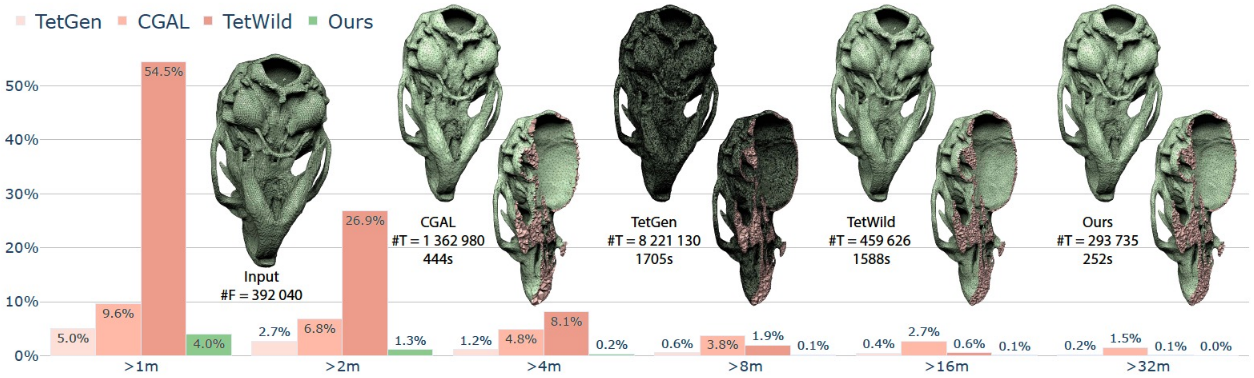

TetWild

CDFEM

A verified conformal decomposition finite element method for implicit, many-material geometries

Scott A. Roberts*, Hector Mendoza, Victor E. Brunini, David R. Noble

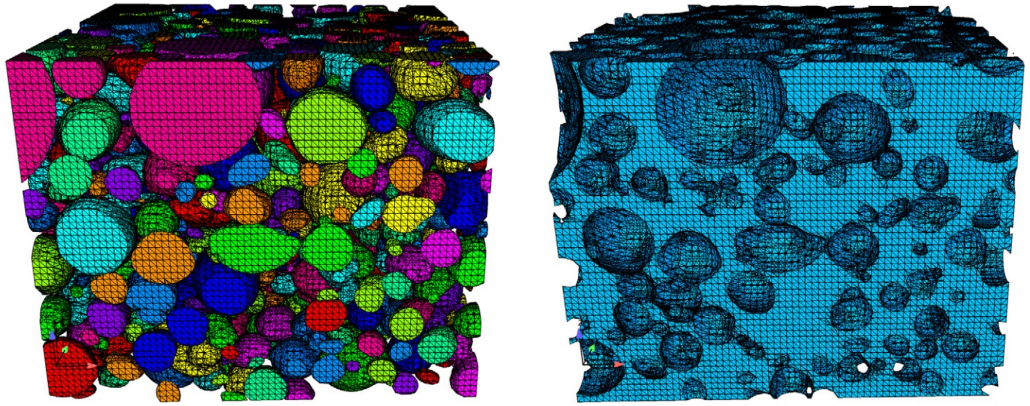

(a) Particles (b) Electrolyte

Hybrid element-free approach

- no defeaturing of domain
- discretize domain using fine-scale triangulation (a mesh, but poor quality is okay)
- use hp-cloud to define solution discretization (GBC, RK)
- use second hp-cloud to define quadrature and ensure coercivity
- projection of solution gradient to obtain polynomial consistency
- visualization of results using fine-scale mesh

pros

- symmetric, Galerkin
- linear or nonlinear
- implicit or explicit dynamics
- can do higher order
- can do direct or mixed formulation
- adaptivity is seamless
- can use poor quality tet mesh
- adaptivity is facilitated
- should work for H(div) and H(curl) spaces
- reduced order modeling through coarse discretizations

cons

- constant material properties within a domain
- material interfaces: have to use weak enforcement such as mortar method
- less sparse

Hybrid element-free approach

INTERNATIONAL JOURNAL FOR NUMERICAL METHODS IN ENGINEERING, VOL. 37, 229–256 (1994)

ELEMENT-FREE GALERKIN METHODS

T. BELYTSCHKO, Y. Y. LU AND L. GU

Department of Civil Engineering, Robert R. McCormick School of Engineering and Applied Science, The Technological Institute, Northwestern University, Evanston IL 60208-3109, U.S.A.

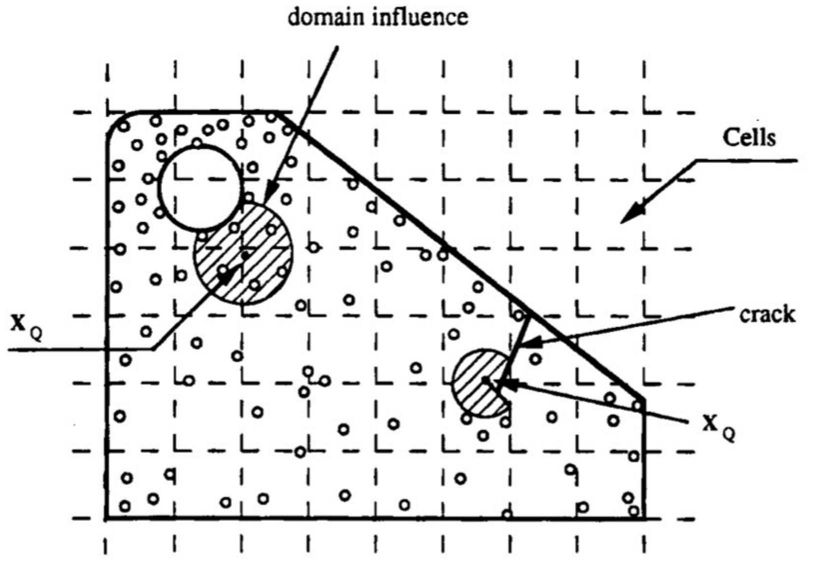

Figure 1. Cell structure for quadrature in EFGM and domains of quadrature point

Moving Least Squares (Reproducing Kernel)

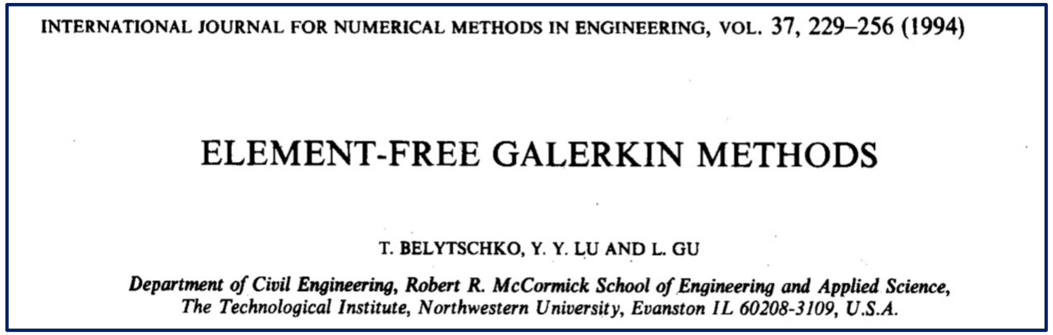
INTERNATIONAL JOURNAL FOR NUMERICAL METHODS IN ENGINEERING, VOL. 37, 229–256 (1994)

ELEMENT-FREE GALERKIN METHODS

T. BELYTSCHKO, Y. Y. LU AND L. GU

Department of Civil Engineering, Robert R. McCormick School of Engineering and Applied Science, The Technological Institute, Northwestern University, Evanston IL 60208-3109, U.S.A.

The MLS shape functions $\phi_I(\mathbf{X})$ are defined as a spatial modulation of the nodal weight functions.

$$\phi_I(\mathbf{X}) = c_I(\mathbf{X}) w_I(\mathbf{X})$$

where the modulation function $c_I(\mathbf{X})$ is found through a least square minimization process resulting in

$$c_I(\mathbf{X}) = \mathbf{g}^{\mathrm{T}}(\mathbf{X})\mathbf{A}^{-1}(\mathbf{X})\mathbf{g}(\mathbf{X}_I)$$

where

$$\mathbf{A}(\mathbf{X}) = \sum_{I \in \mathcal{N}} w_I(\mathbf{X})\mathbf{g}(\mathbf{X}_I)\mathbf{g}^{\mathrm{T}}(\mathbf{X}_I)$$ (sum over neighbors)

$$\mathbf{g}^{\mathrm{T}}(\mathbf{X}) = \{\, 1 \;\, X_1 \;\, X_2 \,\}$$ (linear reproducibility)

Note: shape function construction is algebraic.

nodal weight function

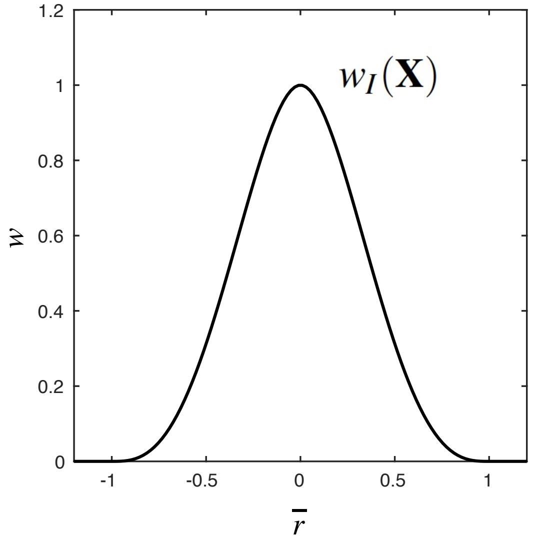

circular or rectangular support

Moving Least Squares

$$\sum_K \phi_K(x) = 1$$

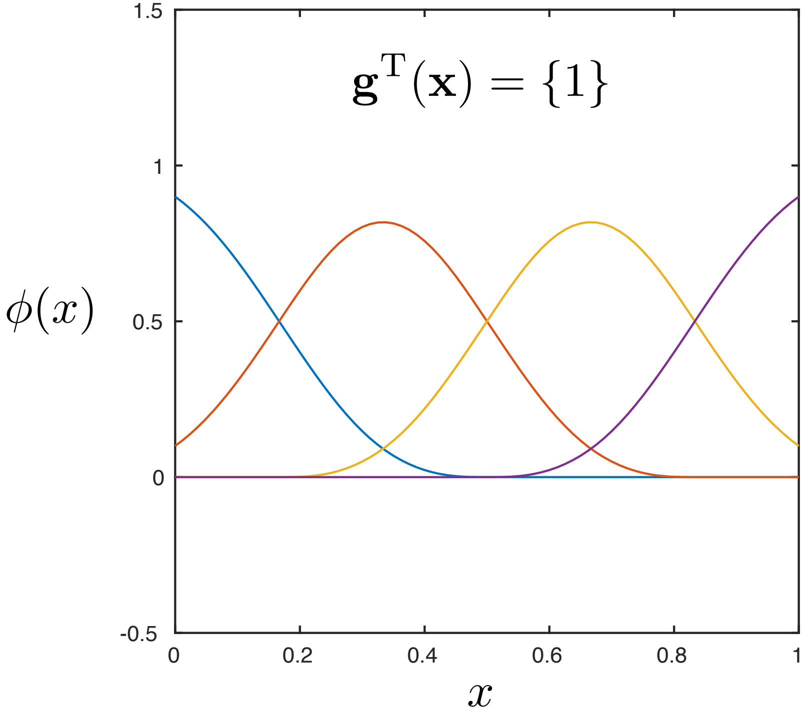

$$\sum_K \phi_K(x) = 1$$

$$\sum_K x_K \, \phi_K(x) = x$$

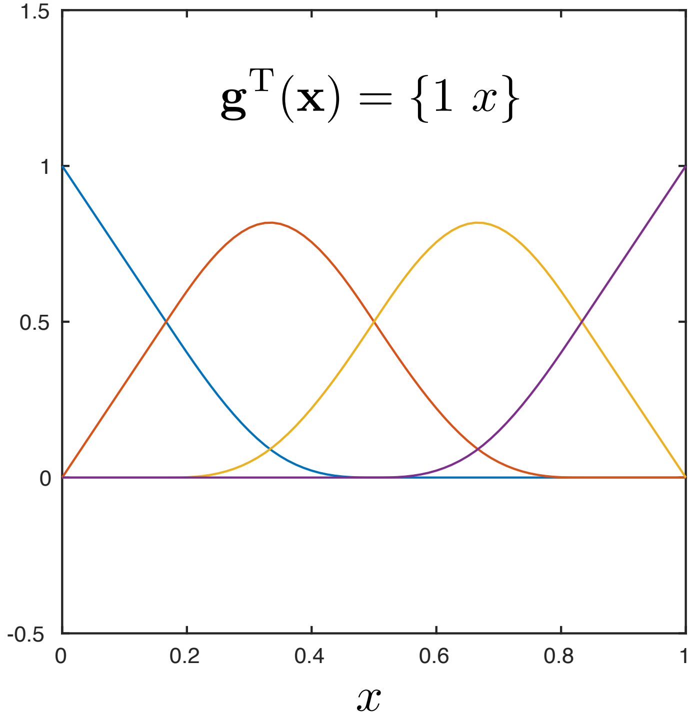

$$\sum_K \phi_K(x) = 1$$

$$\sum_K x_K \, \phi_K(x) = x$$

$$\sum_K x_K^2 \, \phi_K(x) = x^2$$

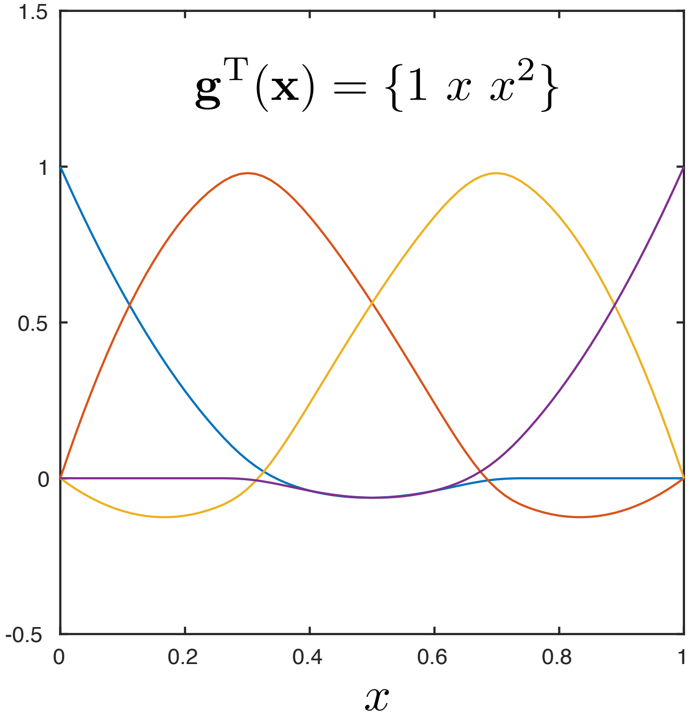

Computational Mechanics 18 (1996) 225–235 © Springer-Verlag 1996

Continuous meshless approximations for nonconvex bodies by diffraction and transparency

D. Organ, M. Fleming, T. Terry, T. Belytschko

domain with slot

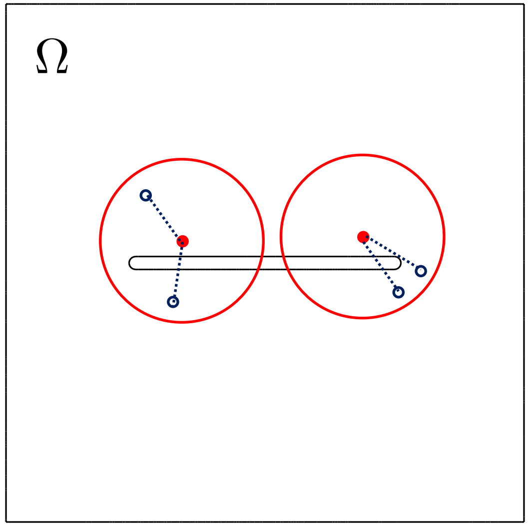

visibility criterion

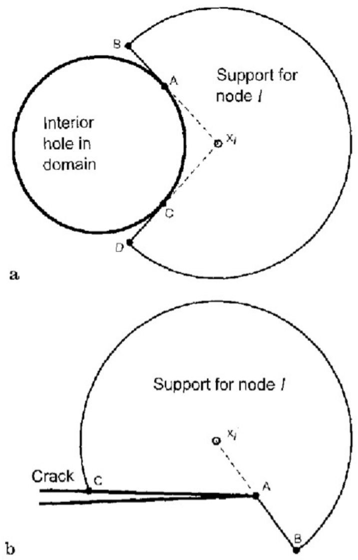

Fig. 1a,b. Domains of influence near nonconvex boundaries using the *visibility criterion* **a** Supportnear a hole, **b** Support near a crack tip

visibility criterion

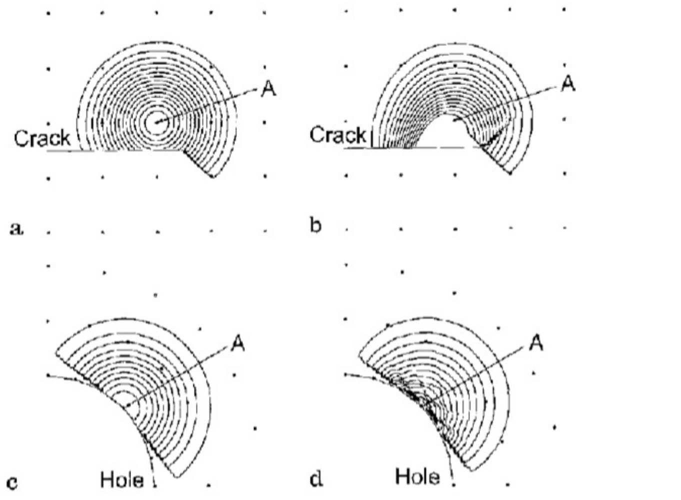

Fig. 2a–d. Contours for weight and shape functions associated with node A constructed using the *visibility criterion*. **a** Weight function near a crack tip, **b** Shape function near a crack tip, **c** Weight function near a hole, **d** Shape function near a hole

All these methods (visibility, transparency, diffraction) require use of computational geometry.

Computational Mechanics 18 (1996) 225–235 © Springer-Verlag 1996

Continuous meshless approximations for nonconvex bodies by diffraction and transparency

D. Organ, M. Fleming, T. Terry, T. Belytschko

diffraction method

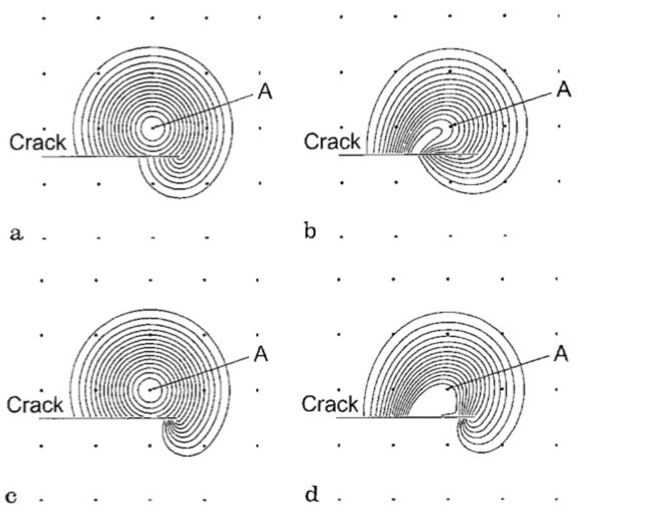

Fig. 5a–d. Contours for weight and shape functions associated with node A near a crack tip constructed using the *diffraction method.* The quartic weight function in (2.18b) was used with $d_{max} = 2.01$ **a** Weight function for $\lambda = 1$, **b** Shape function for $\lambda = 1$, **c** Weight function for $\lambda = 2$, **d** Shape function for $\lambda = 2$

transparancy method

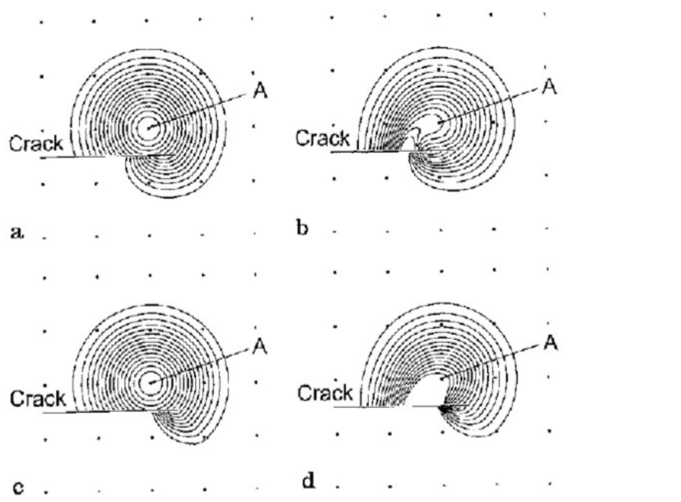

Fig. 8a–d. Contours for weight and shape functions associated with node A near a crack tip constructed using the *transparency method.* The quartic weight function in (2.18b) was used with $d_{max} = 2.01$. **a** Weight function for $\kappa = 1.0$, **b** Shape function for $\kappa = 1.0$, **c** Weight function for $\kappa = 0.5$, **d** Shape function for $\kappa = 0.5$

All these methods (visibility, transparency, diffraction) require use of computational geometry.

Manifold geodesic

Geodesic: path that provides the shortest distance along a manifold

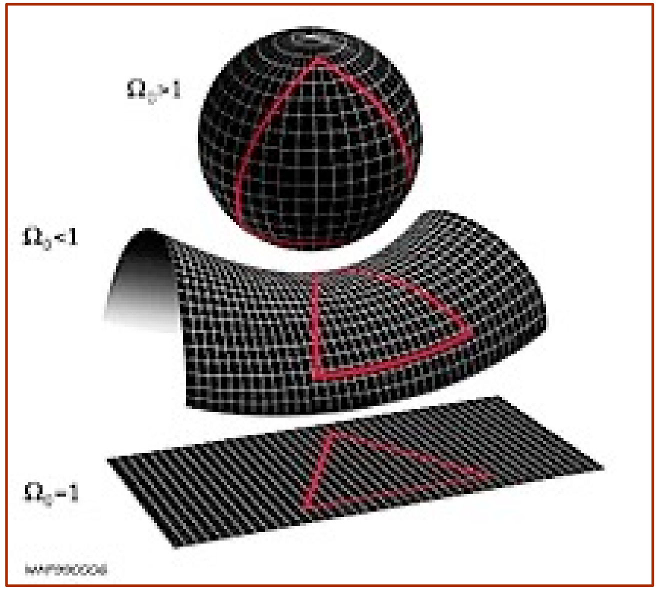

https://en.wikipedia.org/wiki/Geodesic

Euclidean manifold with boundary

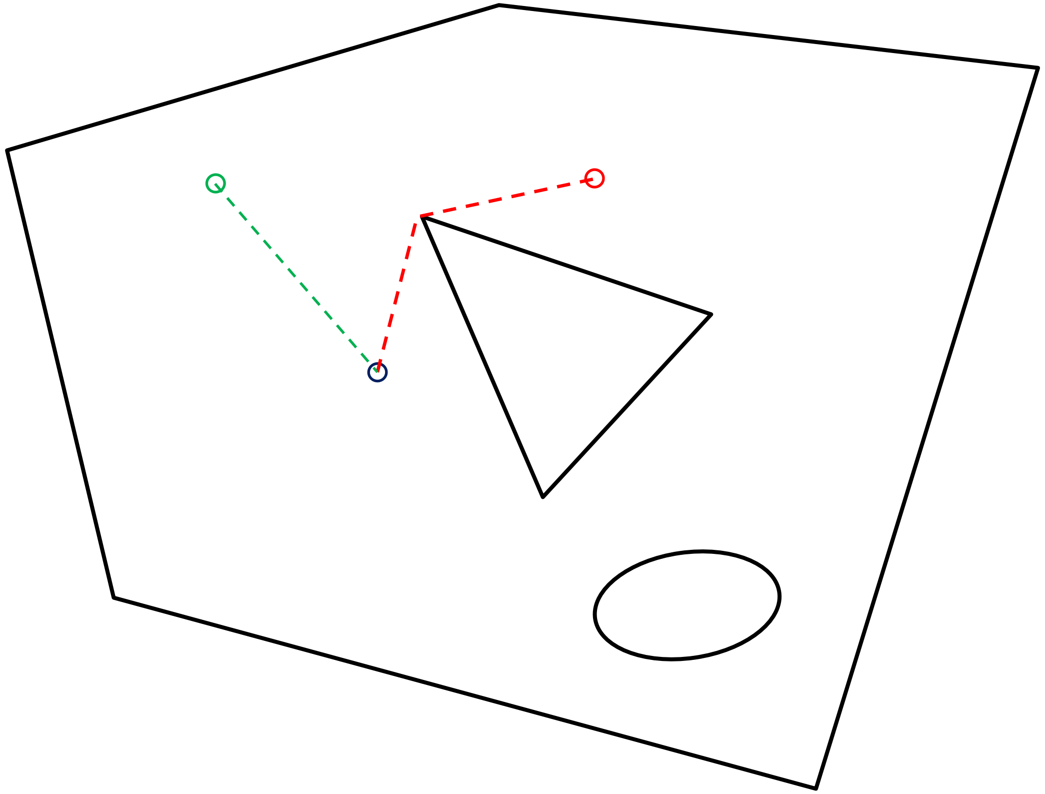

Geodesics in Heat: A New Approach to Computing Distance Based on Heat Flow

KEENAN CRANE
Caltech
and
CLARISSE WEISCHEDEL and MAX WARDETZKY,
University of Göttingen

ACM Trans. Graph. 2013 Vol. 32 Issue 5 Pages Article 152

ALGORITHM 1: The Heat Method

I. Integrate the heat flow $\dot{u} = \Delta u$ for some fixed time t.
II. Evaluate the vector field $X = -\nabla u / |\nabla u|$.
III. Solve the Poisson equation $\Delta \phi = \nabla \cdot X$.

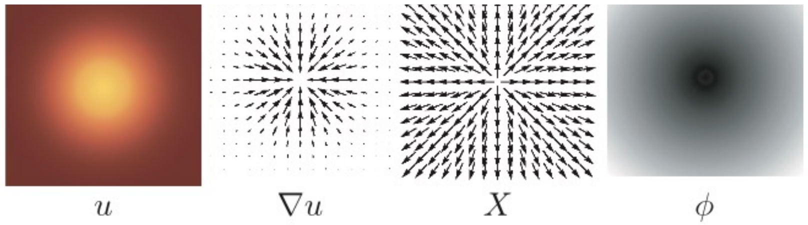

Fig. 5. Outline of the heat method. (I) Heat u is allowed to diffuse for a brief period of time *(left)*. (II) The temperature gradient ∇u *(center left)* is normalized and negated to get a unit vector field X *(center right)* pointing along geodesics. (III) A function ϕ whose gradient follows X recovers the final distance *(right)*.

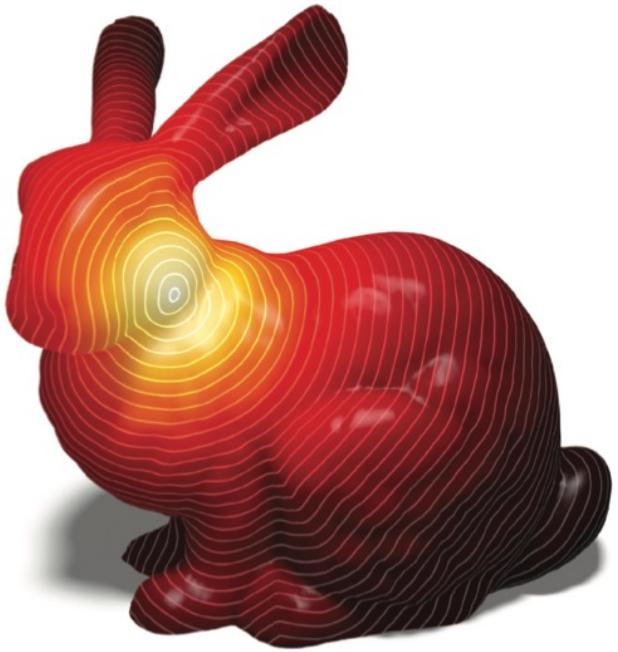

Fig. 1. Geodesic distance from a single point on a surface. The heat method allows distance to be rapidly updated for new source points or curves.

Weight functions using heat flow

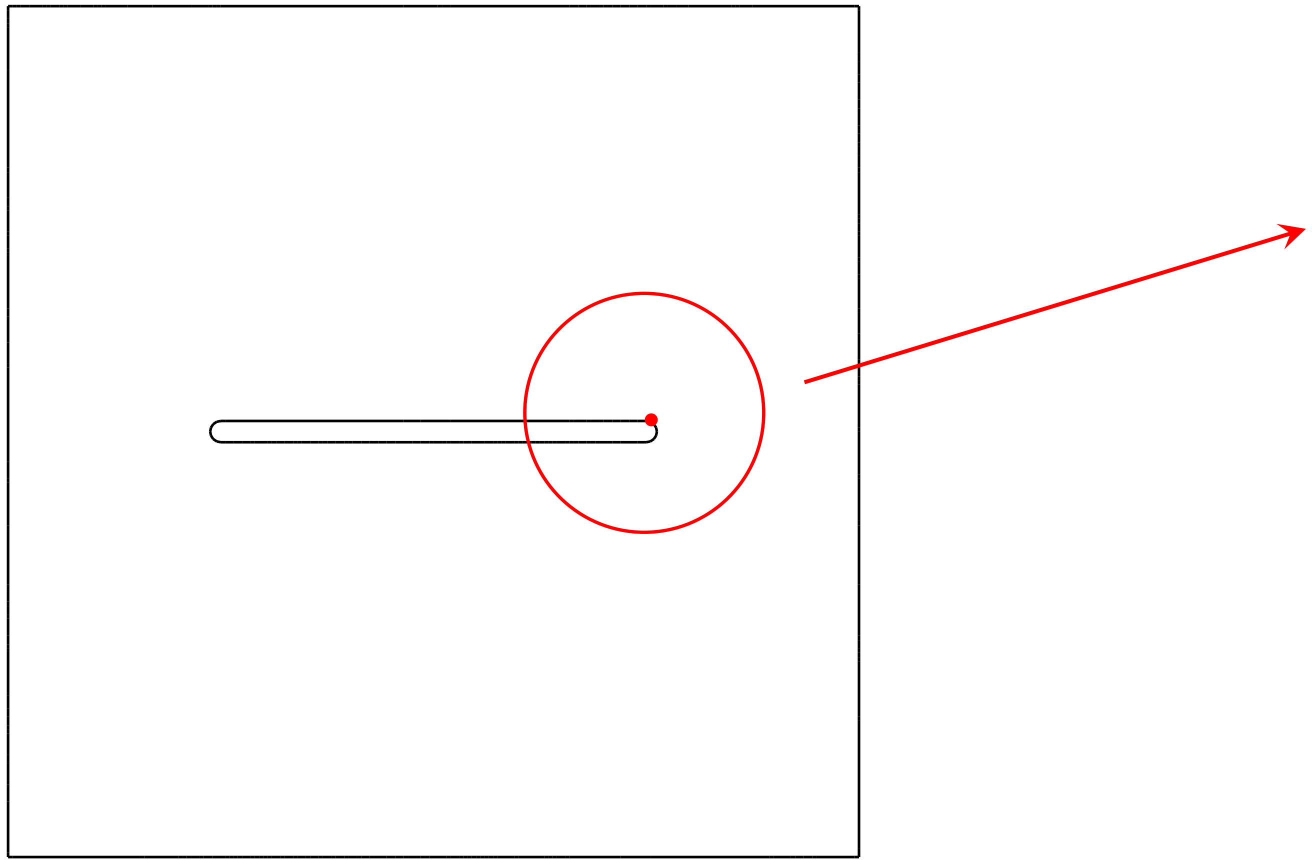

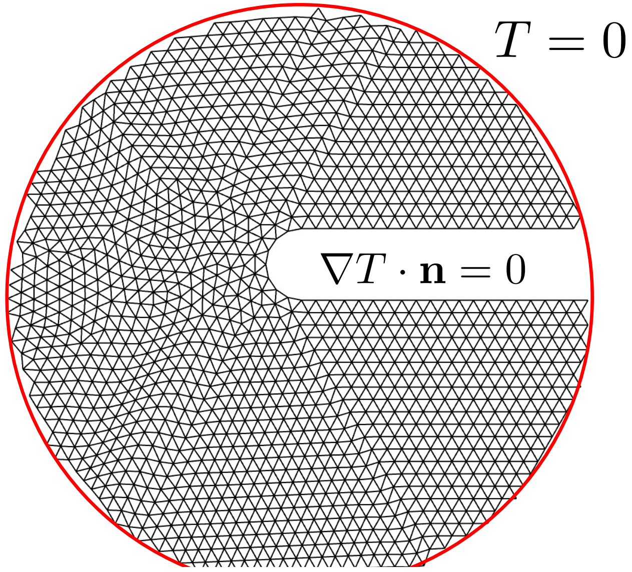

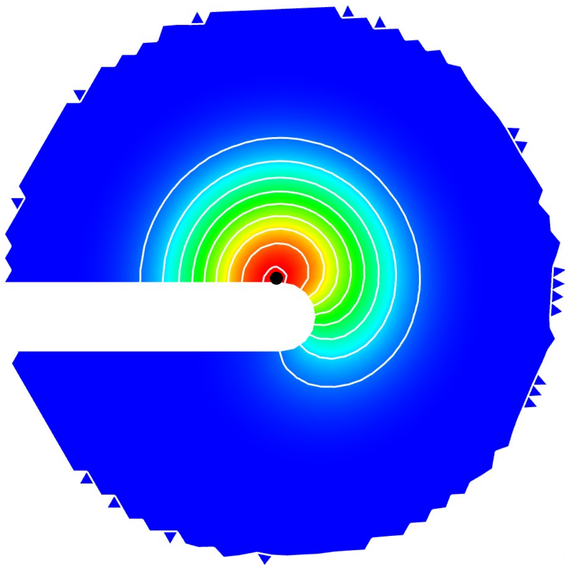

Weight functions using heat flow

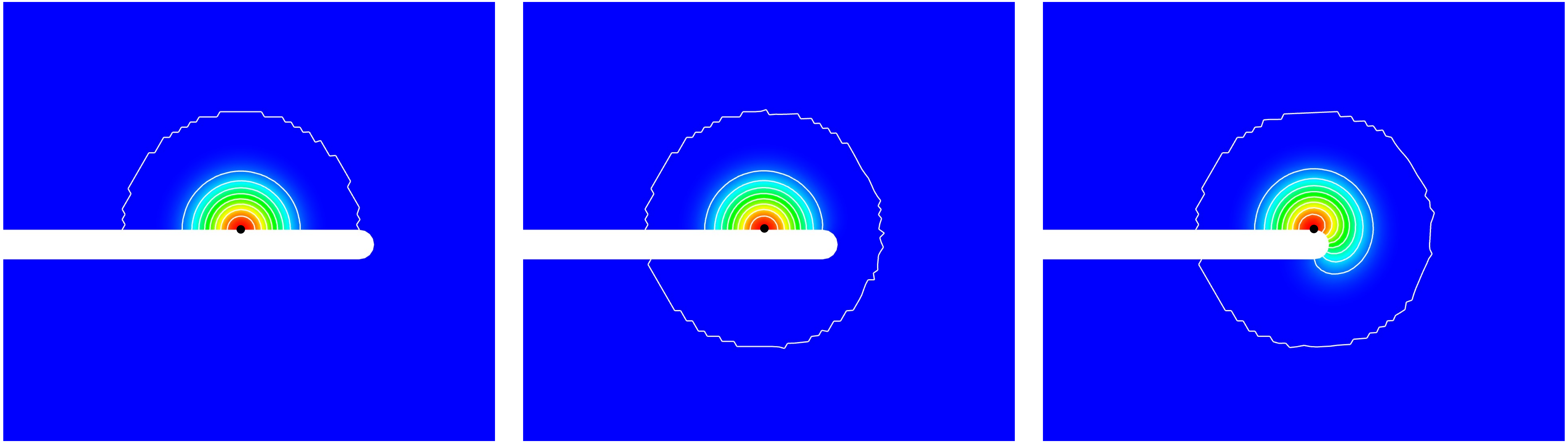

Node placement

- uniform on boundary
- random close packing on interior (maximal Poisson sampling)

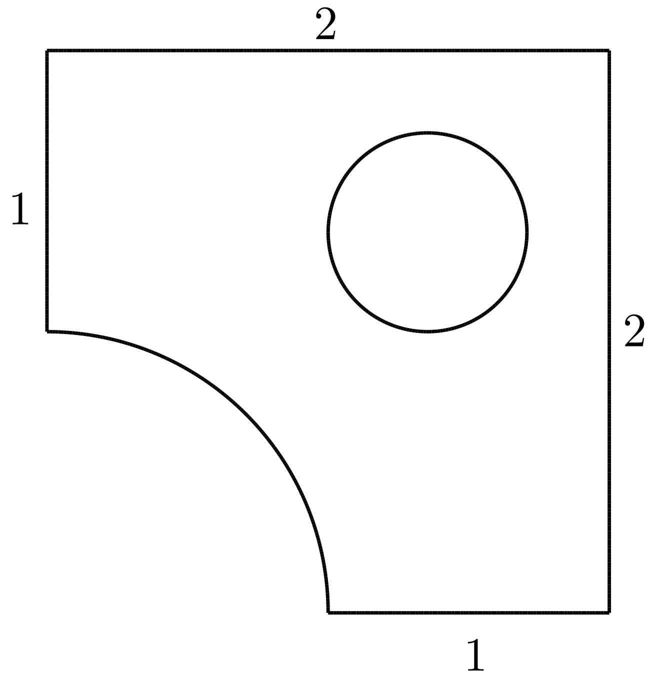

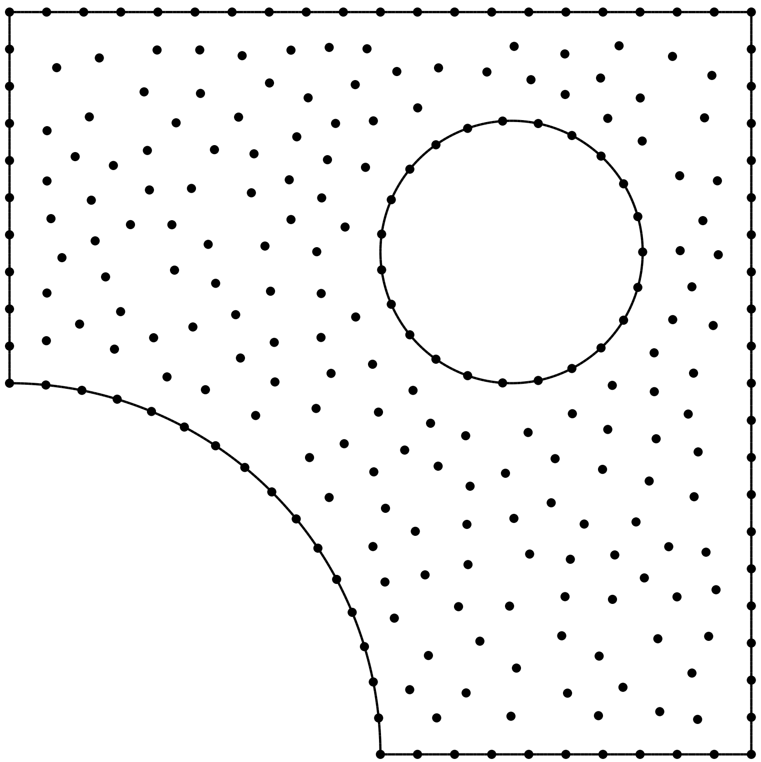

packing size:

$$H = 0.1$$

Weight function support size

support size

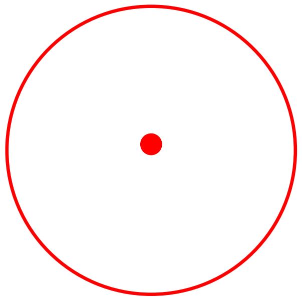

encloses underlying tri mesh

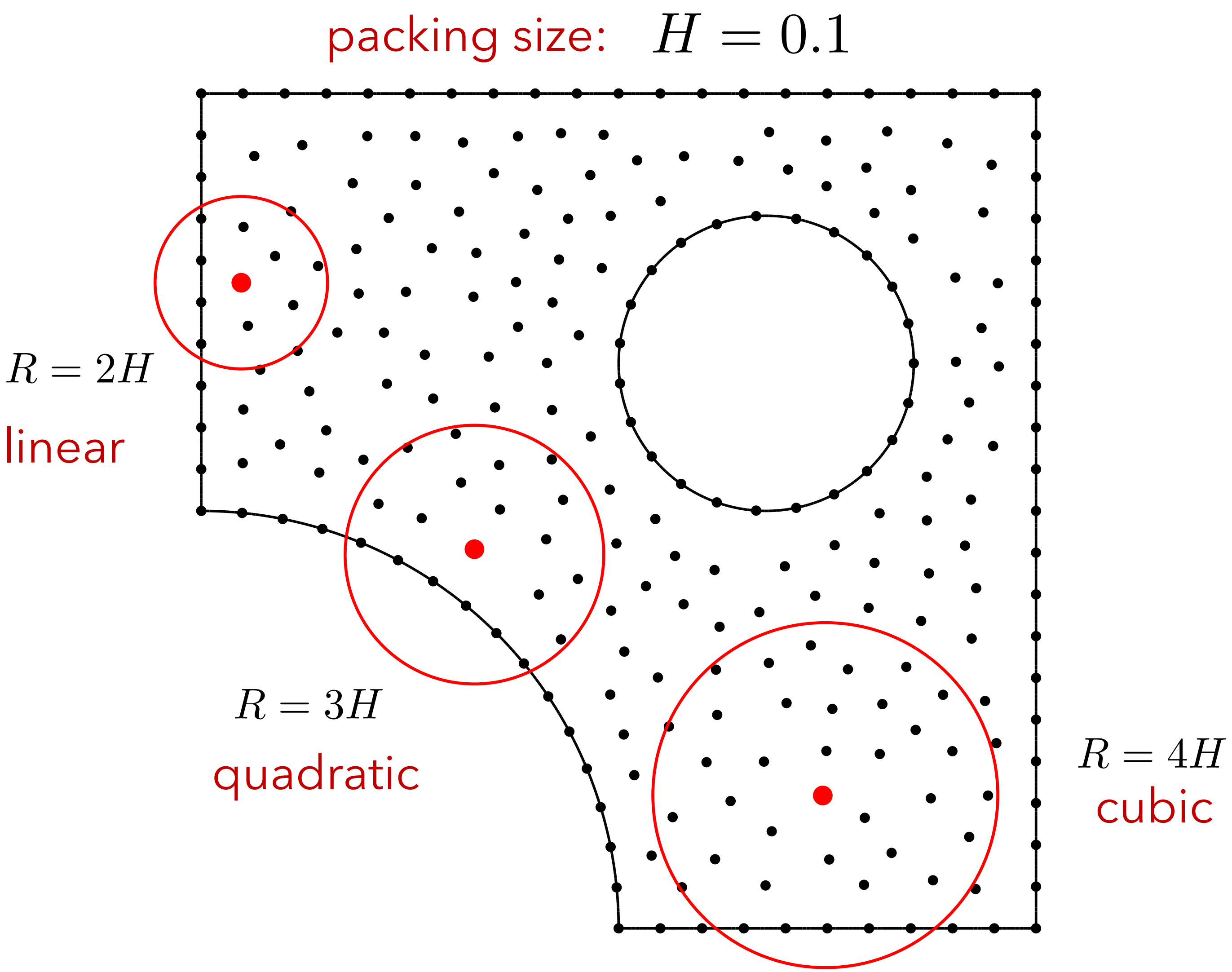

weight functions

shape functions (basis)

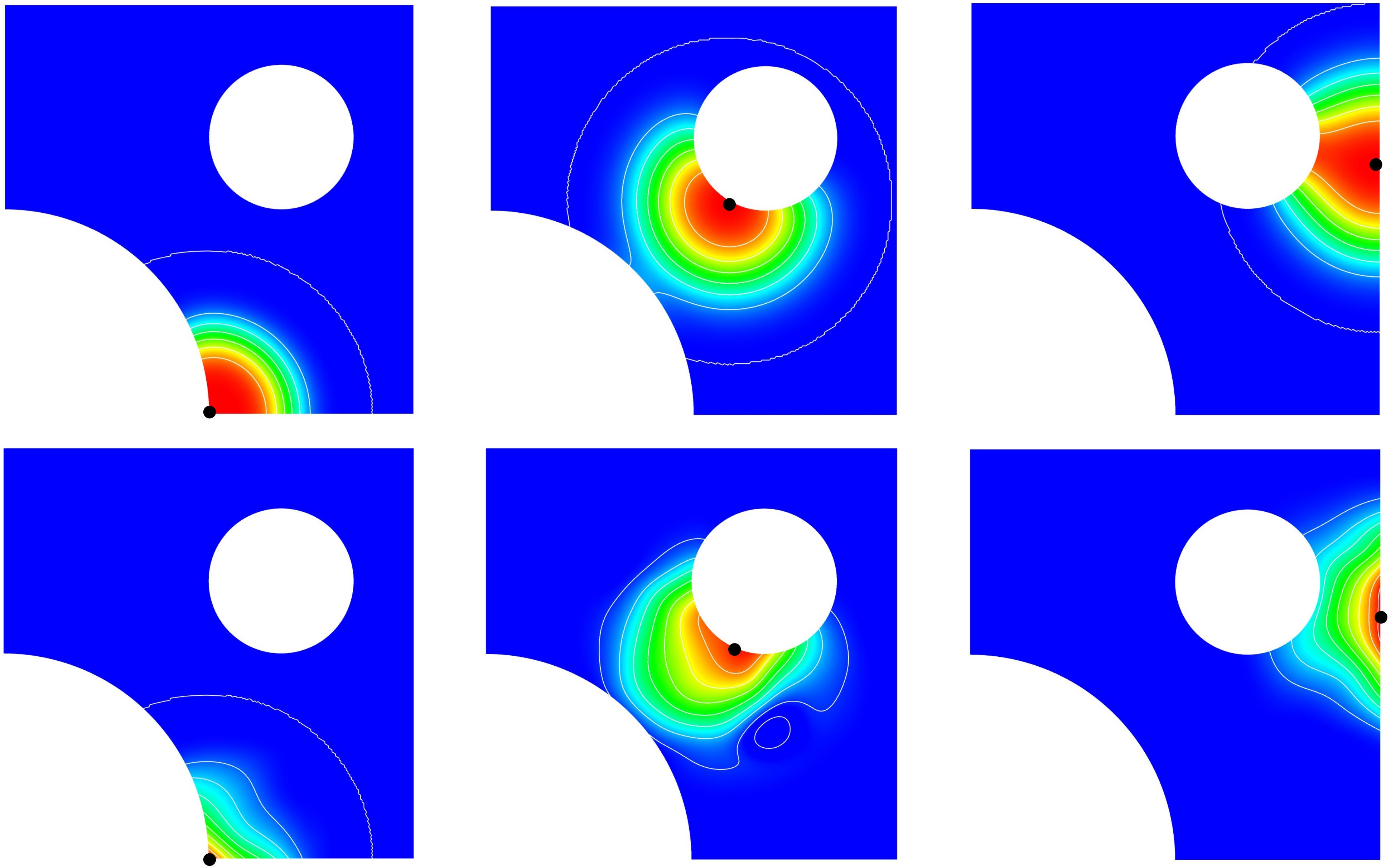

How to do quadrature?

Observe that partition-of-unity property allows us to approximate any continuous function arbitrarily closely using only point evaluations as long as basis functions have local support.

Given $\sum_K \phi_K(\mathbf{x}) = 1$ then it follows that $f(\mathbf{x}) \approx \sum_K f(\mathbf{x}_K)\phi_K(\mathbf{x}) := f_h(\mathbf{x})$ *non-interpolatory approximation*

Theorem: For every $\varepsilon > 0$ and $\mathbf{x} \in \overline{\Omega}$, there exists $h(\varepsilon) > 0$ such that $|\, f_h(\mathbf{x}) - f(\mathbf{x}) \,| < \varepsilon$.

It follows that $\int f(\mathbf{x})\, d\Omega \approx \int f_h(\mathbf{x})\, d\Omega$

with $\left| \int f_h(\mathbf{x})\, d\Omega - \int f(\mathbf{x})\, d\Omega \right| \leq \int |\, f_h(\mathbf{x}) - f(\mathbf{x}) \,|\, d\Omega \leq \int \varepsilon\, d\Omega = V \cdot \varepsilon$

Can obtain rates of convergence using Taylor's theorem.

Approximation property

let $f(x) = |2x - 1|\sqrt{x}$

$$f_N = \sum_{K=1}^{N} f(x_K)\phi_K(x)$$

function approximation

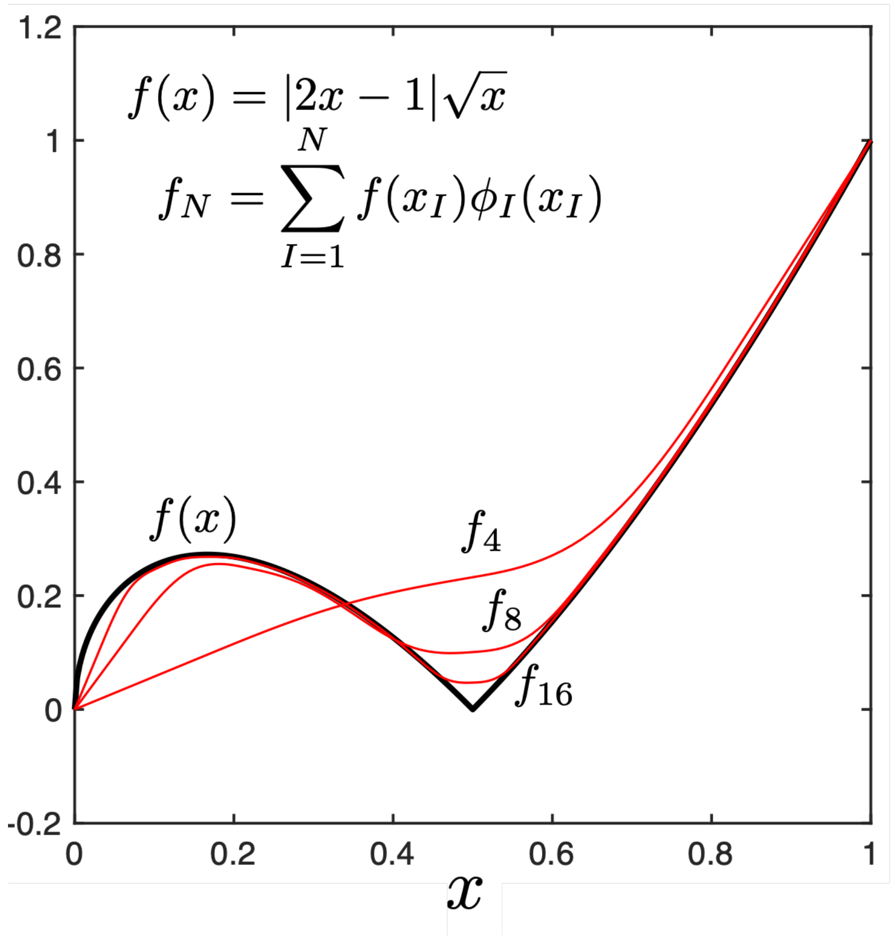

Quadrature

$$\int f(\mathbf{x})\, d\Omega \approx \int f_h(\mathbf{x})\, d\Omega = \int \sum_K f(\mathbf{x}_K)\phi_K(\mathbf{x})\, d\Omega = \sum_K f(\mathbf{x}_K) \int \phi_K(\mathbf{x})\, d\Omega$$

Define quadrature weight as $\mathrm{w}_K = \int_\Omega \phi_K(\mathbf{x})\, d\Omega$

$$\int f(\mathbf{x})\, d\Omega \approx \sum_K \mathrm{w}_K f(\mathbf{x}_K)$$

Can show that $\sum_K \mathrm{w}_K = V$ and $\sum_K \mathrm{w}_K \, \mathbf{x}_K = \int_\Omega \mathbf{x}\, d\Omega$

Now have a second-order integration scheme that can integrate linear functions exactly.

Quadrature

Note that $$\sum_K \mathrm{w}_K = \sum_K \int_\Omega \phi_K(\mathbf{x})\, d\Omega = \int_\Omega \sum_K \phi_K(\mathbf{x})\, d\Omega = \int_\Omega 1\, d\Omega = V$$

Also, since $$\sum_K \mathbf{x}_K\, \phi_K(\mathbf{x}) = \mathbf{x}$$

then $$\sum_K \mathrm{w}_K \mathbf{x}_K = \sum_K \int_\Omega \phi_K(\mathbf{x})\, \mathbf{x}_K\, d\Omega = \int_\Omega \sum_K \mathbf{x}_K \phi_K(\mathbf{x})\, d\Omega = \int_\Omega \mathbf{x}\, d\Omega$$

Now have a second-order integration scheme that can integrate linear functions exactly.

$$\sum_K \mathrm{w}_K = V \qquad\qquad \sum_K \mathrm{w}_K\, \mathbf{x}_K = \int_\Omega \mathbf{x}\, d\Omega$$

Can extend to higher-order integration using higher-order reproducing conditions.

Quadrature example

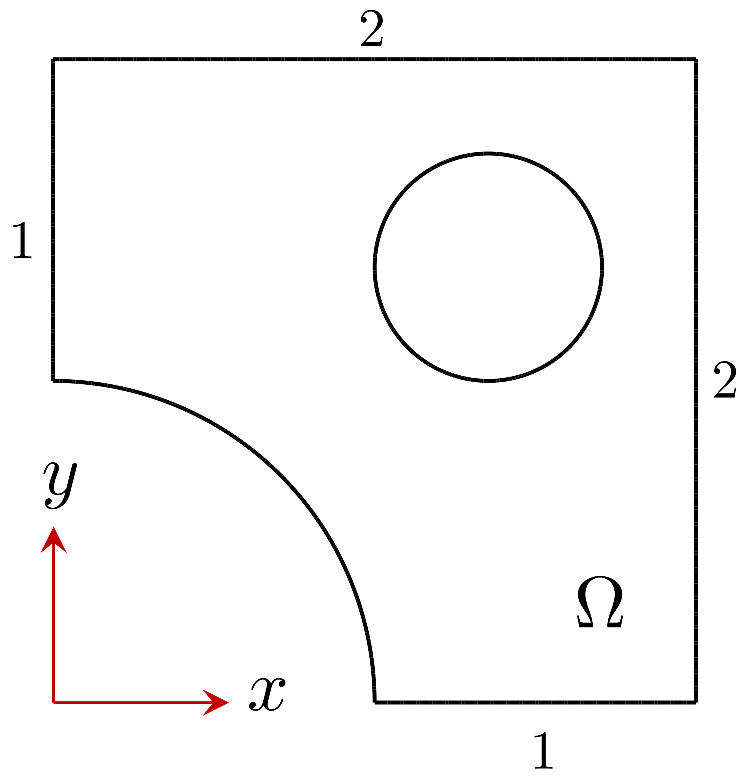

$$f(x, y) = \sin(\pi x/2)\sin(\pi y)$$

$$\text{error} := \left| \sum_K \mathrm{w}_K f(\mathbf{x}_K) - \int_\Omega f \, d\Omega \right|$$

Quadrature example

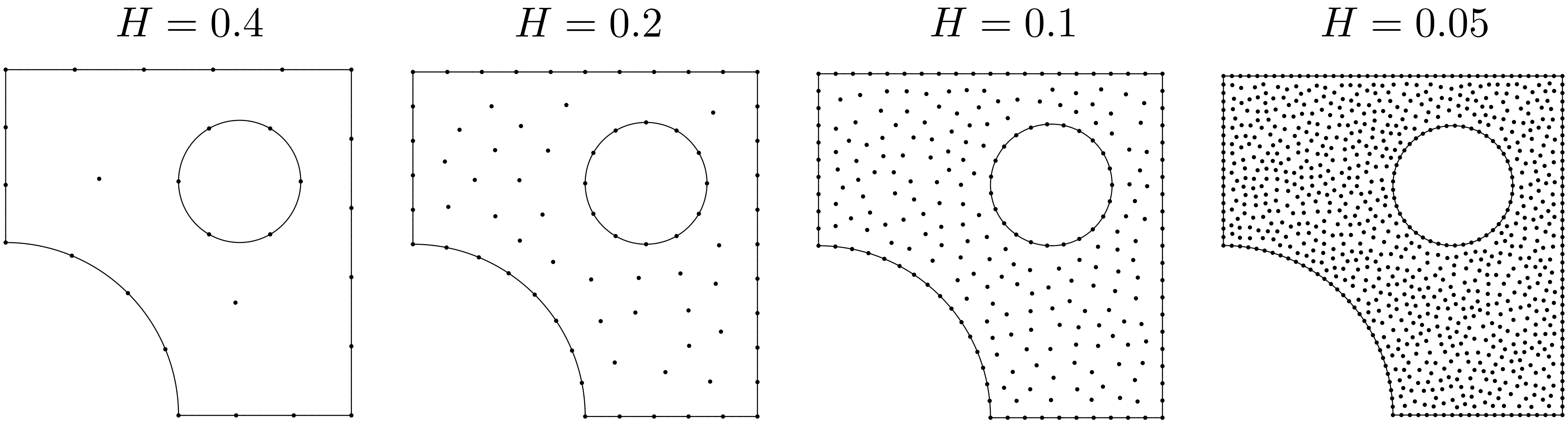

Evaluate error for 10 realizations.

Quadrature weights

$$\mathrm{w}_K = \int_\Omega \phi_K(\mathbf{x})$$

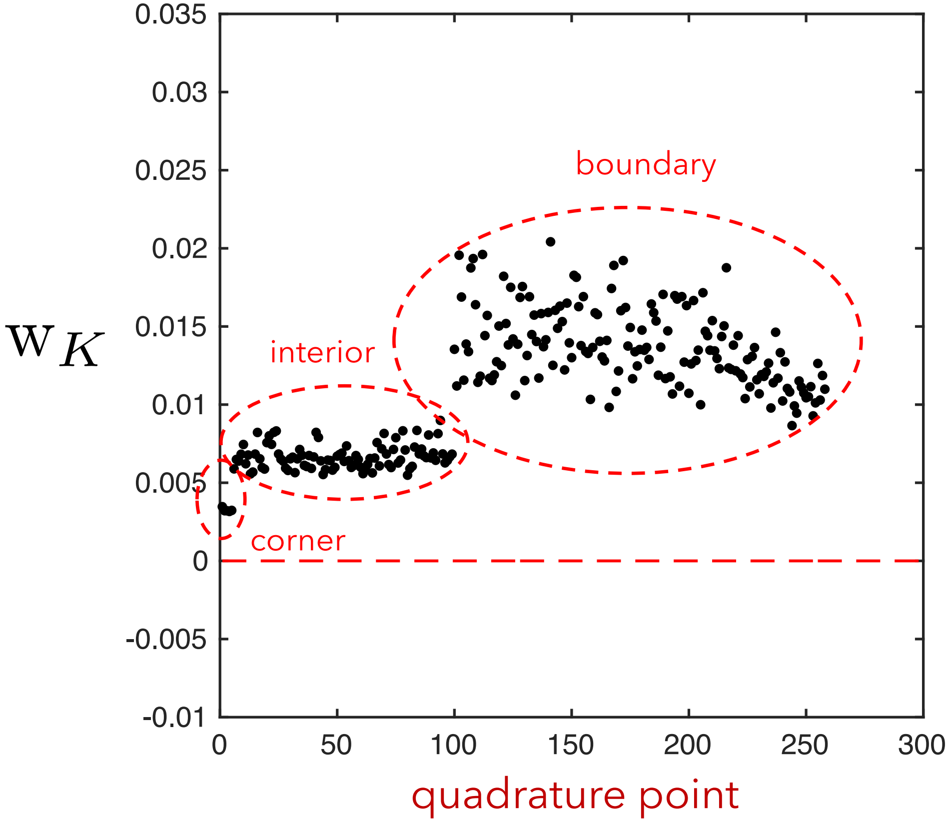

$$\text{error} := \left| \sum_K \mathrm{w}_K f(\mathbf{x}_K) - \int_\Omega f \, d\Omega \right|$$

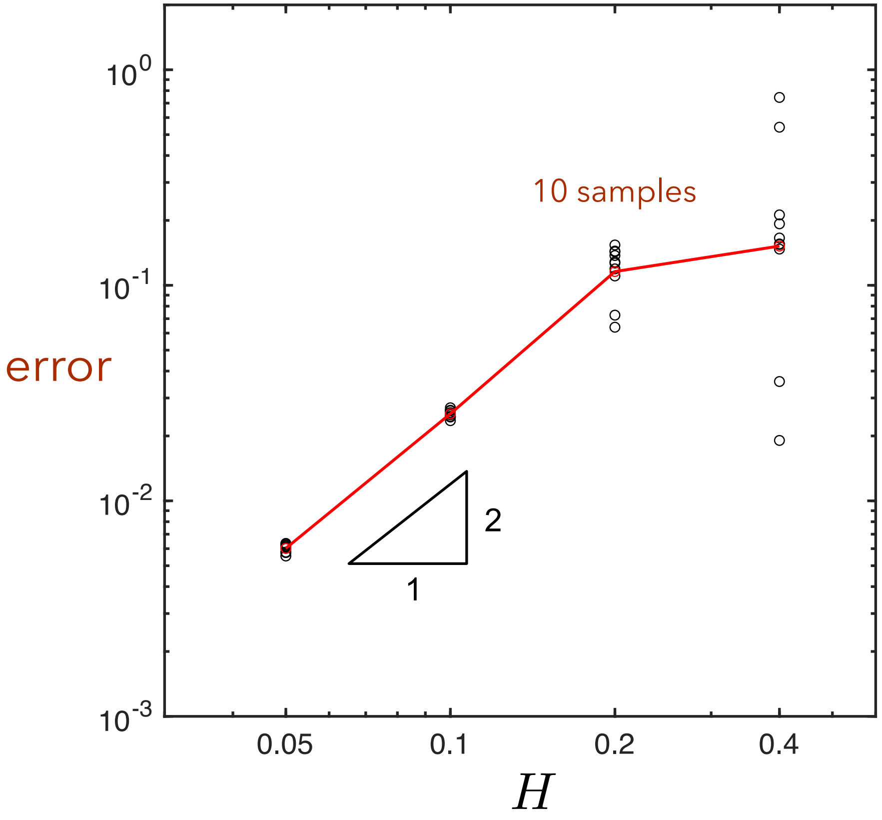

Governing equations for solid mechanics (Lagrangian)

strong form

$$\frac{\partial \boldsymbol{P}}{\partial \boldsymbol{X}} : \boldsymbol{I} = \rho_0\, \ddot{\mathbf{u}}$$

$$\boldsymbol{u} = \overline{\boldsymbol{u}} \quad \text{on} \quad \Gamma_0^u \quad \text{and} \quad \boldsymbol{P} \cdot \boldsymbol{N} = \boldsymbol{t}_0 \quad \text{on} \quad \Gamma_0^t$$

P is first Piola-Kirchhoff stress tensor

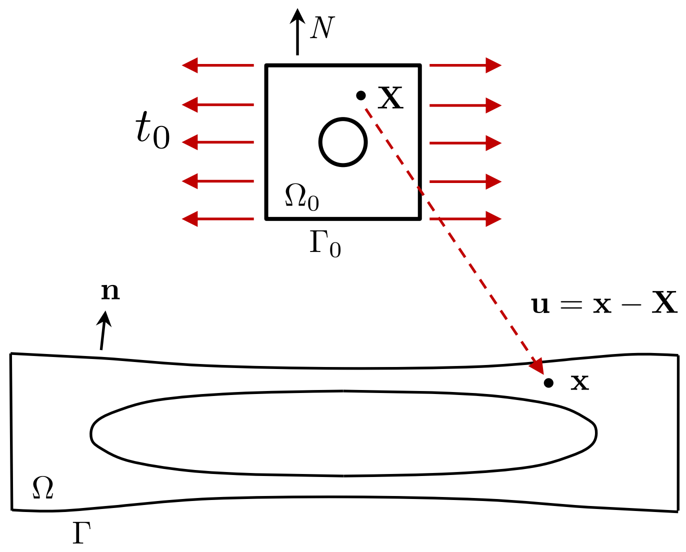

weak form

find the trial functions $\boldsymbol{u} \in \boldsymbol{H}^1(\Omega_0)$ such that

$$\int_{\Gamma_0^t} \boldsymbol{t}_0 \cdot \boldsymbol{v}\, dS - \int_{\Omega_0} \boldsymbol{P} : (\partial \boldsymbol{v} / \partial \boldsymbol{X})\, d\boldsymbol{X} = \int_{\Omega_0} \rho_0\, \ddot{\mathbf{u}} \cdot \boldsymbol{v}\, d\boldsymbol{X}$$

for all test functions $\boldsymbol{v} \in \boldsymbol{H}_0^1(\Omega_0)$

Element-free approach to solve BVPs

Use two meshfree clouds: one for solution discretization (DoF) and one for quadrature.

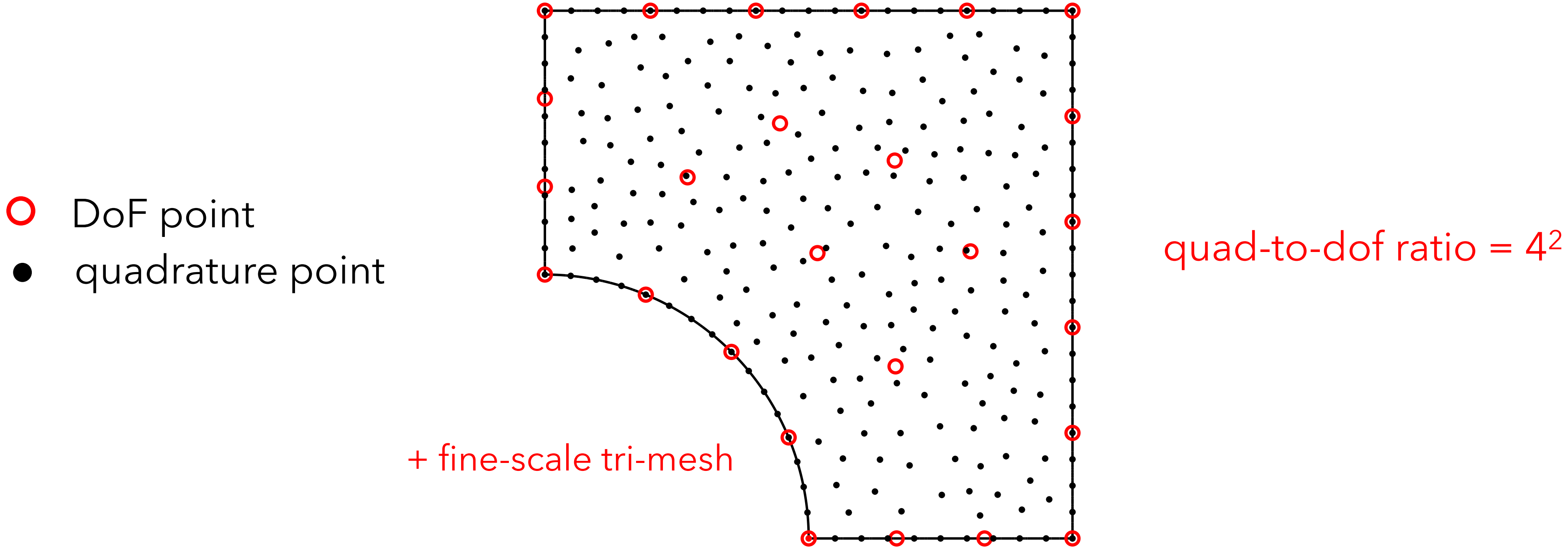

What ratio of quad points to dof points is needed for stability (coercivity of bilinear form)?

Patch test (linear consistency)

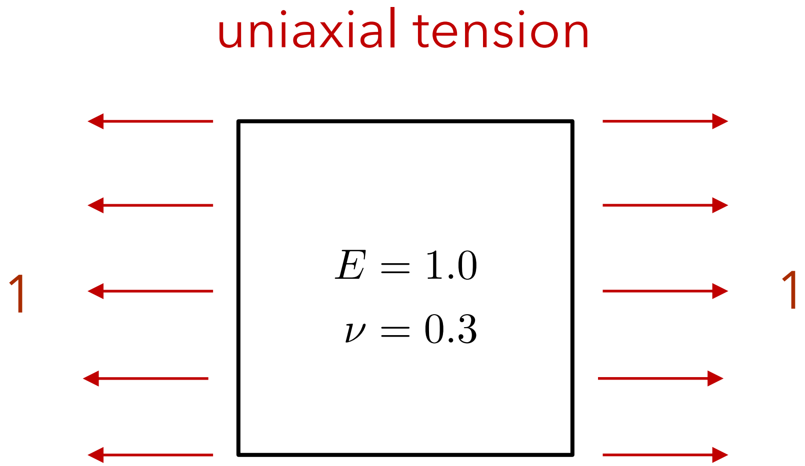

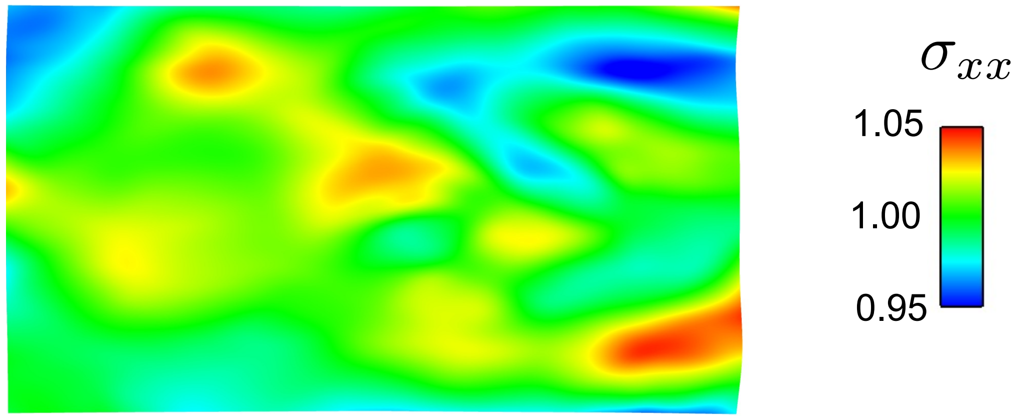

error $> 5\%$

Consistency of discrete form (integration)

- For convergence of discrete approximation, need to ensure consistency of discrete and continuous bilinear forms.
- Requires polynomial consistency of shape-function gradients (including quadrature).
- To obtain quadrature consistency, project the DoF shape function gradients to the subspace of quadrature shape functions.
- Only performed once in a pre-processing step.

$\{\phi_I, I = 1, \ldots, N\}$ *DoF basis (shape functions)*

$\{\Phi_K, K = 1, \ldots, M\}$ *Quadrature basis (shape functions)*

$$\overline{\nabla}\phi_I := \arg\min \int_\Omega \left(\nabla\phi_I - \sum_{K=1}^{M} a^K \Phi_K \right)^2 d\Omega$$ *(L_2 projection)*

The projection can be written in terms of the dual or conjugate basis $\{\Phi^J\}$

$$(\Phi_K, \Phi^J) = \delta_K^J$$ *bi-orthogonal*

$$\overline{\nabla}\phi_I = \sum_K \underbrace{(\nabla\phi_I, \Phi_K)}_{\text{covariant components}}\Phi^K = \sum_K \underbrace{(\nabla\phi_I, \Phi^K)}_{\text{contravariant components}}\Phi_K$$

covariant components

contravariant components

Can prove polynomial consistency up to the order of the precision of $\{\Phi_K\}$

Theorem: $\int_\Omega \mathbf{p}\,\overline{\nabla}\phi_I\, d\Omega = \int_\Omega \mathbf{p}\,\nabla\phi_I\, d\Omega$ for all $\mathbf{p} \in \mathbb{P}_k(\Omega)$

This ensures satisfaction of the patch test.

Replace the original bilinear form $$a(u,v) = \int_\Omega \nabla u : \mathbb{C}\, \nabla v \, d\Omega$$

with this modified bilinear form $$\overline{a}(u,v) = \int_\Omega \overline{\nabla} u : \mathbb{C}\, \overline{\nabla} v \, d\Omega$$

Note: This modified bilinear form is still symmetric (Bubnov-Galerkin).

$$\overline{a}(u,v) = \int_\Omega \left[\sum_I (\nabla u, \Phi_I) \Phi^I \right] \mathbb{C} \left[\sum_J (\nabla v, \Phi_J) \Phi^J \right] d\Omega$$

$$\overline{a}(u,v) = \sum_{I,J} (\nabla u, \Phi_I)\, \mathbb{C}\, (\nabla v, \Phi_J) \underbrace{\int_{\Omega_e} \Phi^I \Phi^J \, d\Omega}_{G^{IJ}}$$

Can show that $G^{IJ} = (G_{IJ})^{-1}$

where $G_{IJ} = \int_{\Omega_e} \Phi_I \Phi_J \, d\Omega$ is the Gram matrix for the basis $\{\Phi_K\}$

Can show that $\Phi^I = G^{IJ}\Phi_J$ and $\Phi_I = G_{IJ}\Phi^J$

"raising" and "lowering" of indices

$$\overline{a}(u,v) = \sum_{I,J} G^{IJ} (\nabla u, \Phi_I)\, \mathbb{C}\, (\nabla v, \Phi_J) = \sum_K (\nabla u, \Phi^K)\, \mathbb{C}\, (\nabla v, \Phi_K)$$

Looks like a sum over quadrature points.

Since $G^{IJ} = (G_{IJ})^{-1}$ is dense:

Replace G_{IJ} with row-sum lumped version: $G^L_{IJ} := \sum_J G_{IJ} = \mathrm{diag}\{\mathrm{w}_K\}$

where recall $\mathrm{w}_K = \int_\Omega \phi_K(\mathbf{x})\, d\Omega$

Then $\overline{a}(u,v) \to \overline{a}^L(u,v) = \sum_K \frac{1}{\mathrm{w}_K}(\nabla u, \Phi_K)\,\mathbb{C}\,(\nabla v, \Phi_K)$ where $(G^L_{IJ})^{-1} = \mathrm{diag}\left\{\frac{1}{\mathrm{w}_K}\right\}$

Can write $\overline{a}^L(u,v)$ as

$$\overline{a}^L(u,v) = \sum_K \mathrm{w}_K\,(\overline{\nabla} u)_K : \mathbb{C}\,(\overline{\nabla} v)_K$$

where

$$(\overline{\nabla} u)_K := \frac{1}{\mathrm{w}_K}\int_\Omega (\nabla u)\,\Phi_K\, d\Omega$$

which has the form of a discrete derivative at a quadrature point K.

Our discrete bilinear form is now "sparse."

Patch test (linear consistency)

uniaxial tension

no projection

with projection

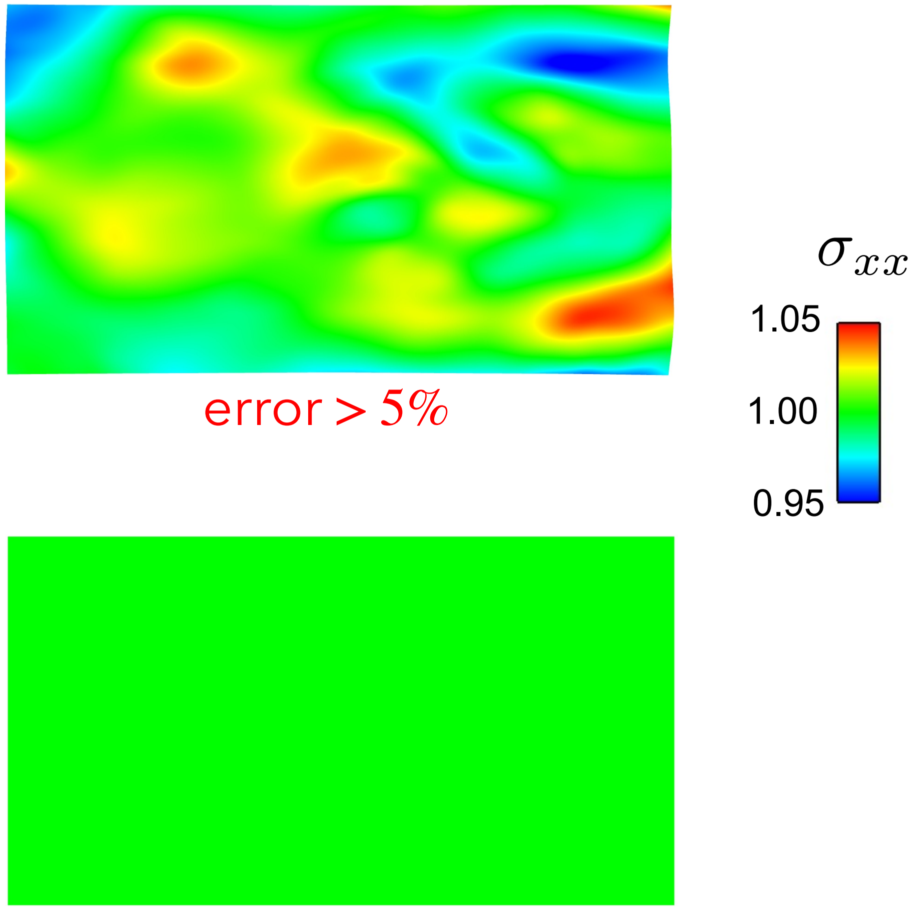

error > 5%

error < 10^{-13}

pure shear

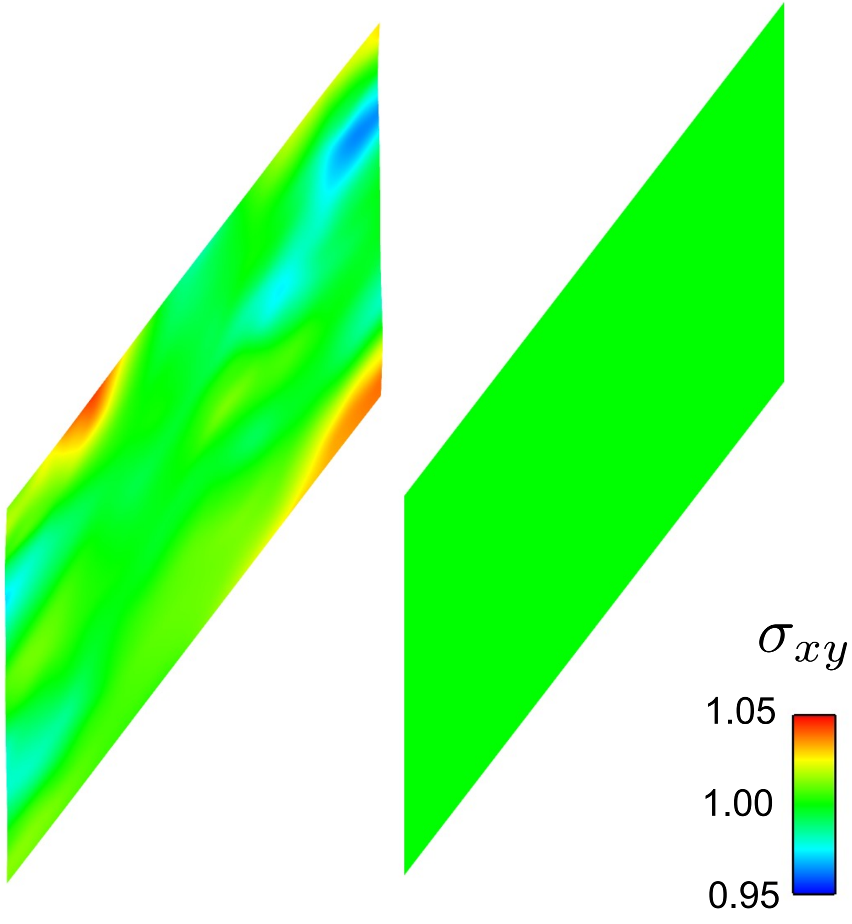

Example: plate with hole

uniaxial tension

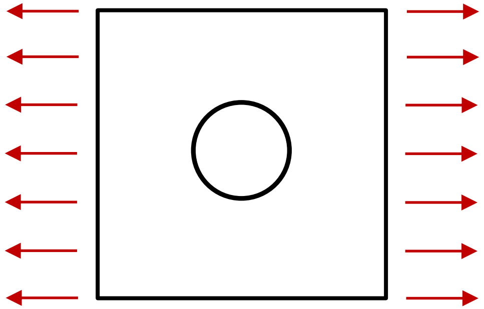

$E = 1.0$

$\nu = 0.3$

exact

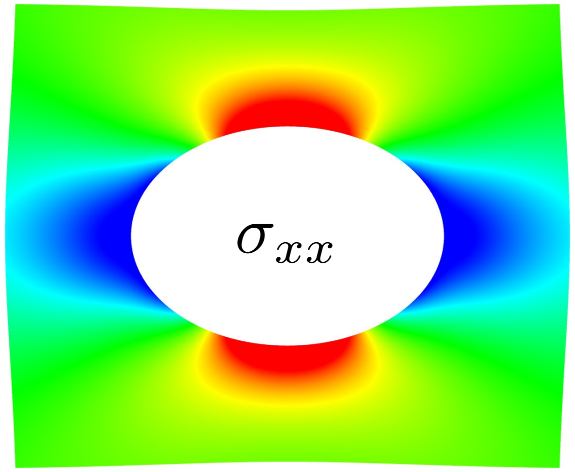

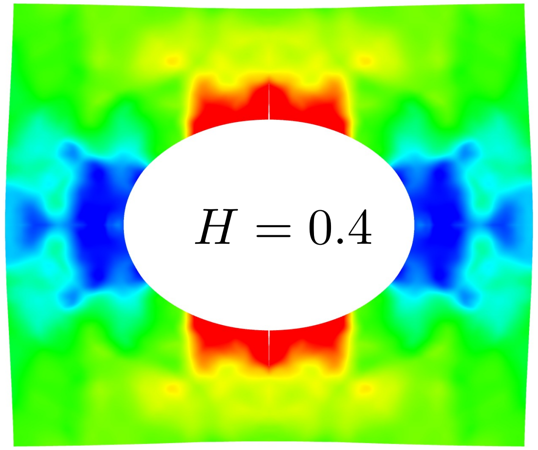

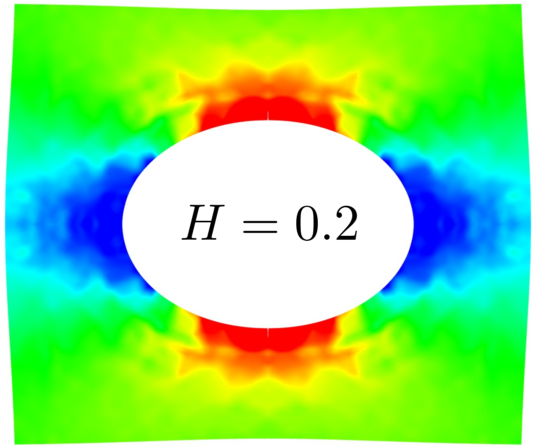

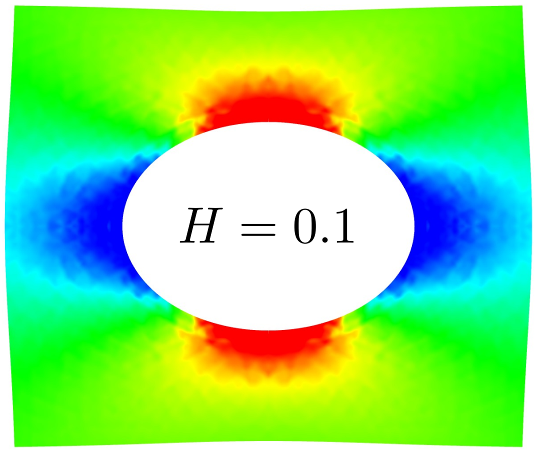

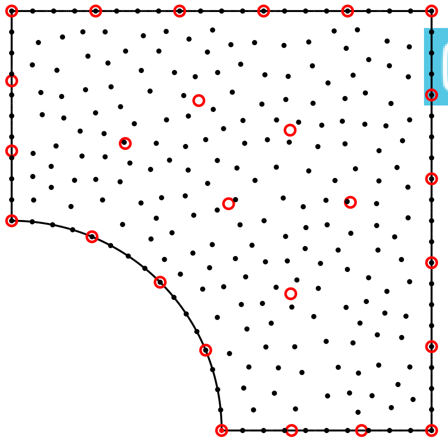

Example: plate with hole

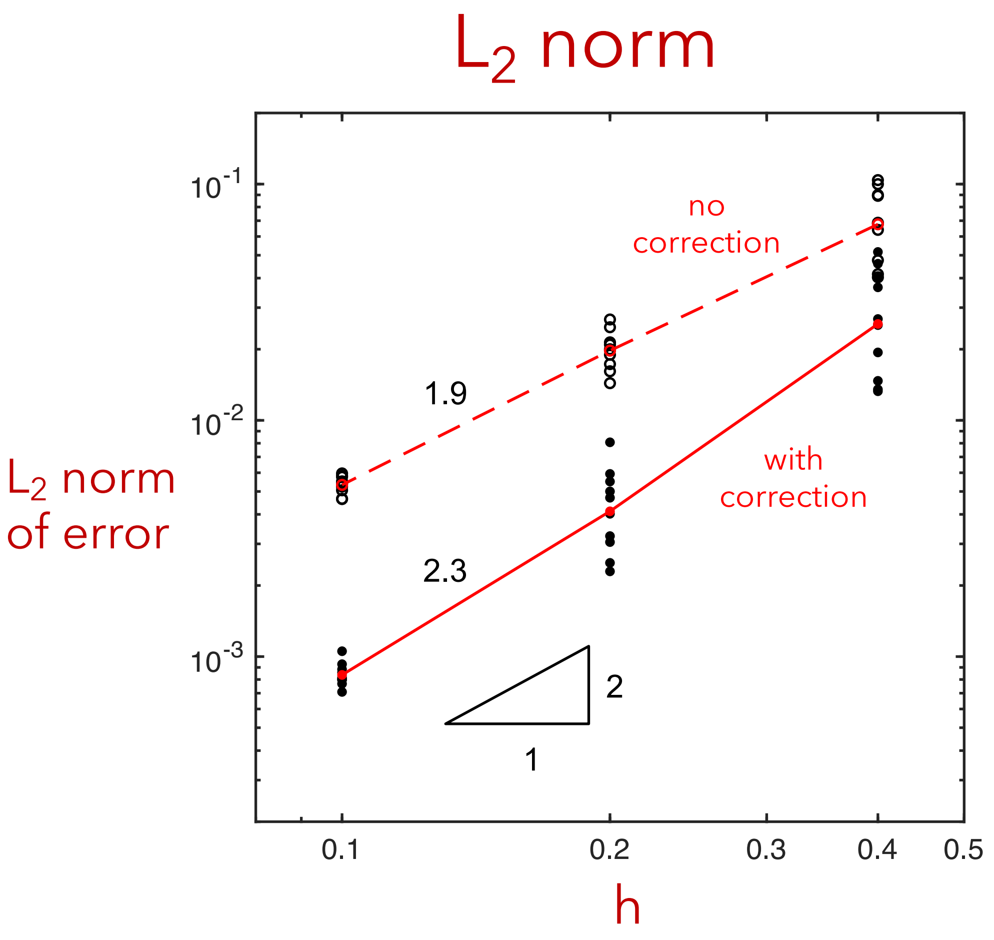

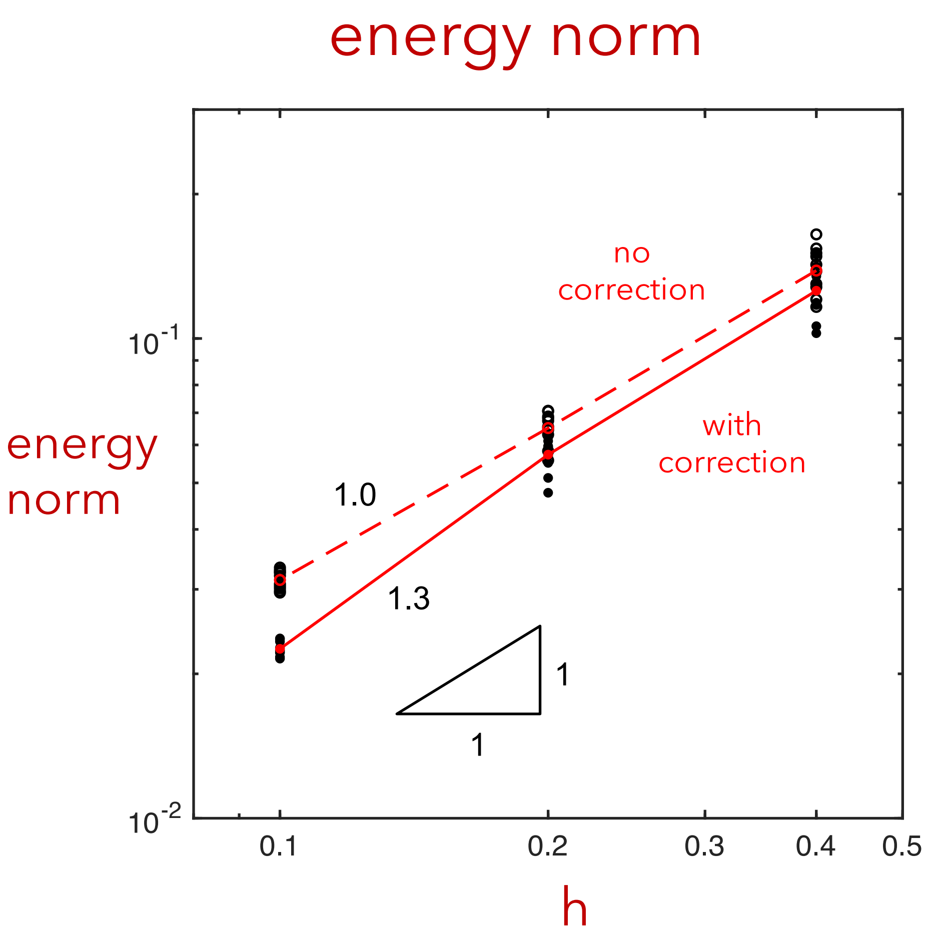

Example

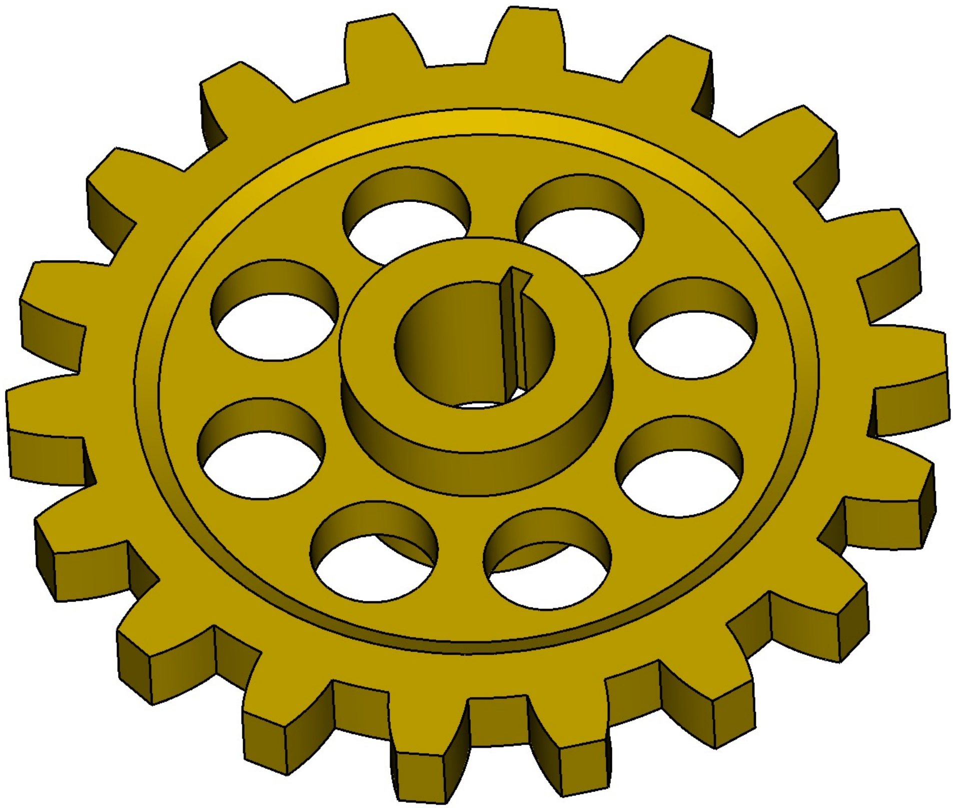

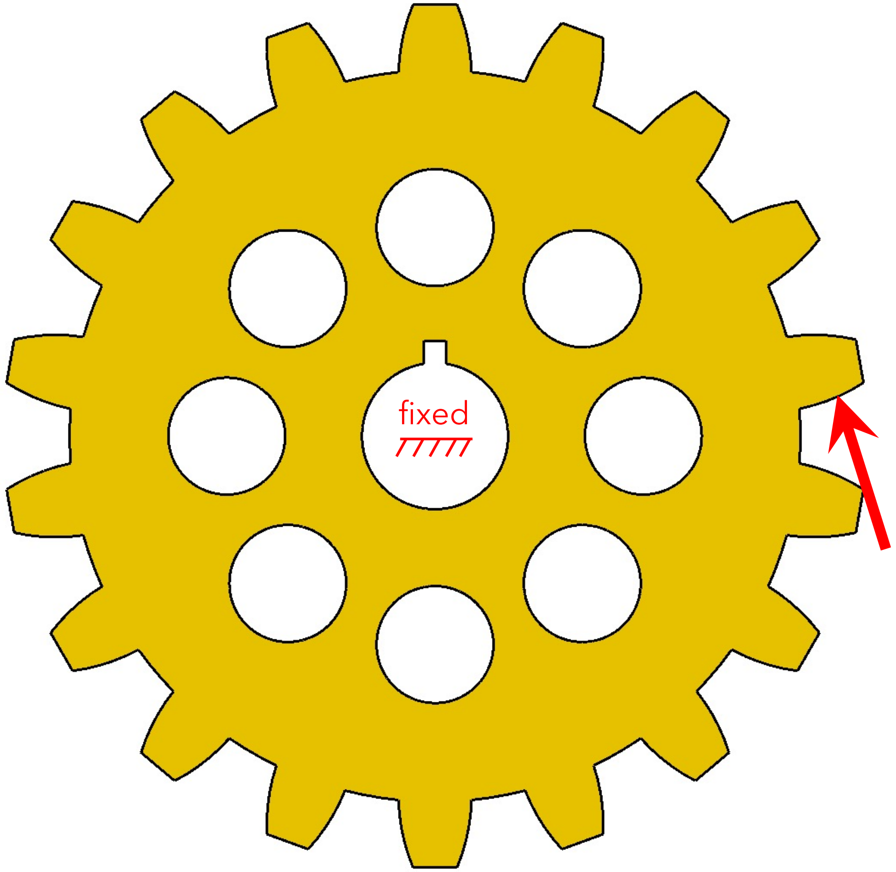

dof nodes

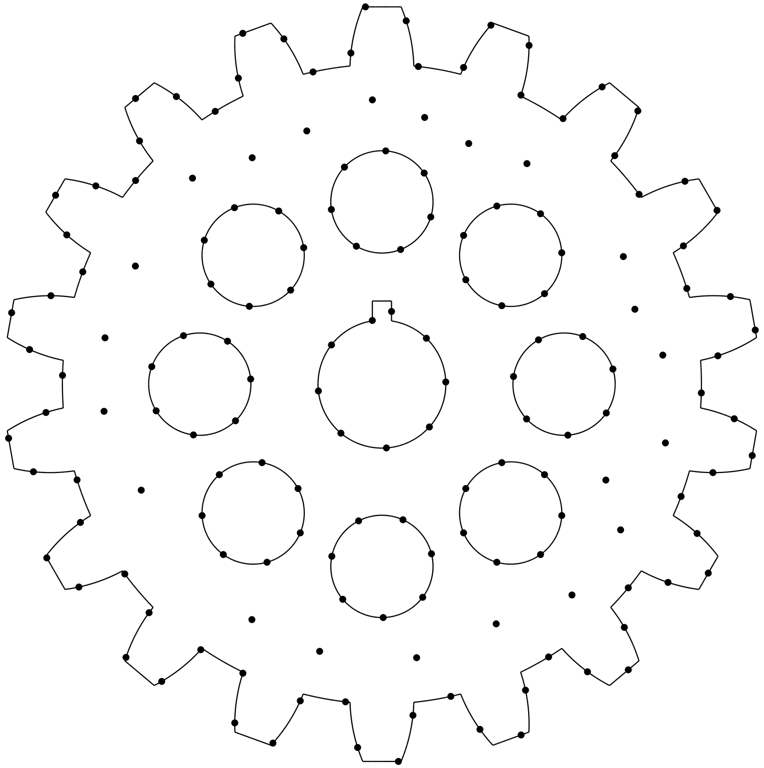

basis functions

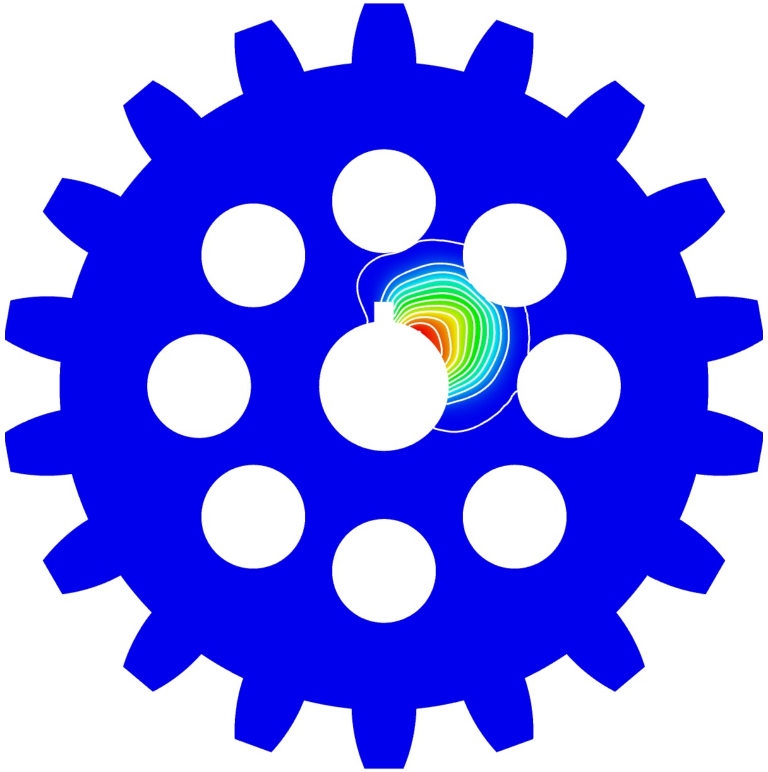

stress field (vm)

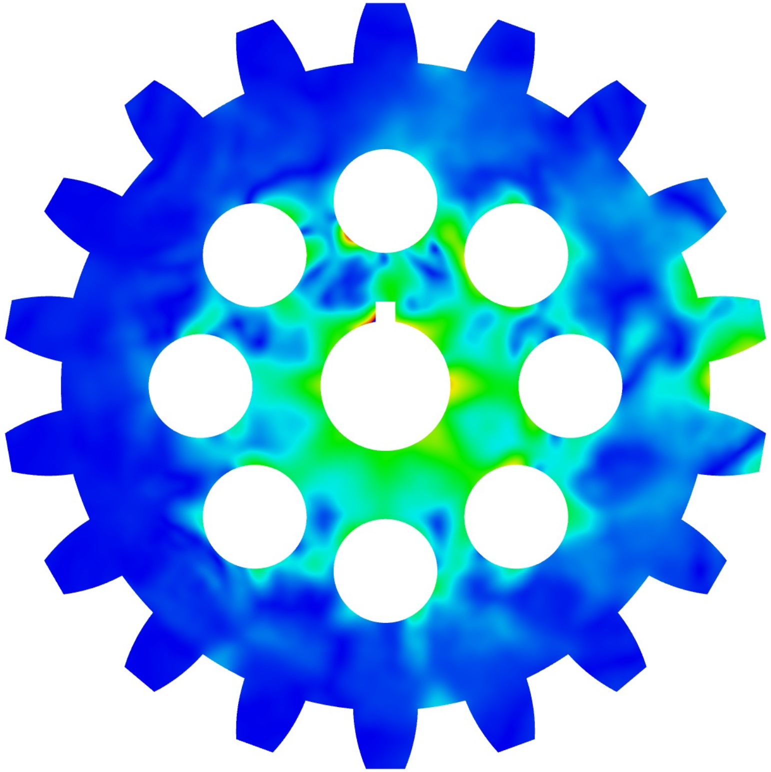

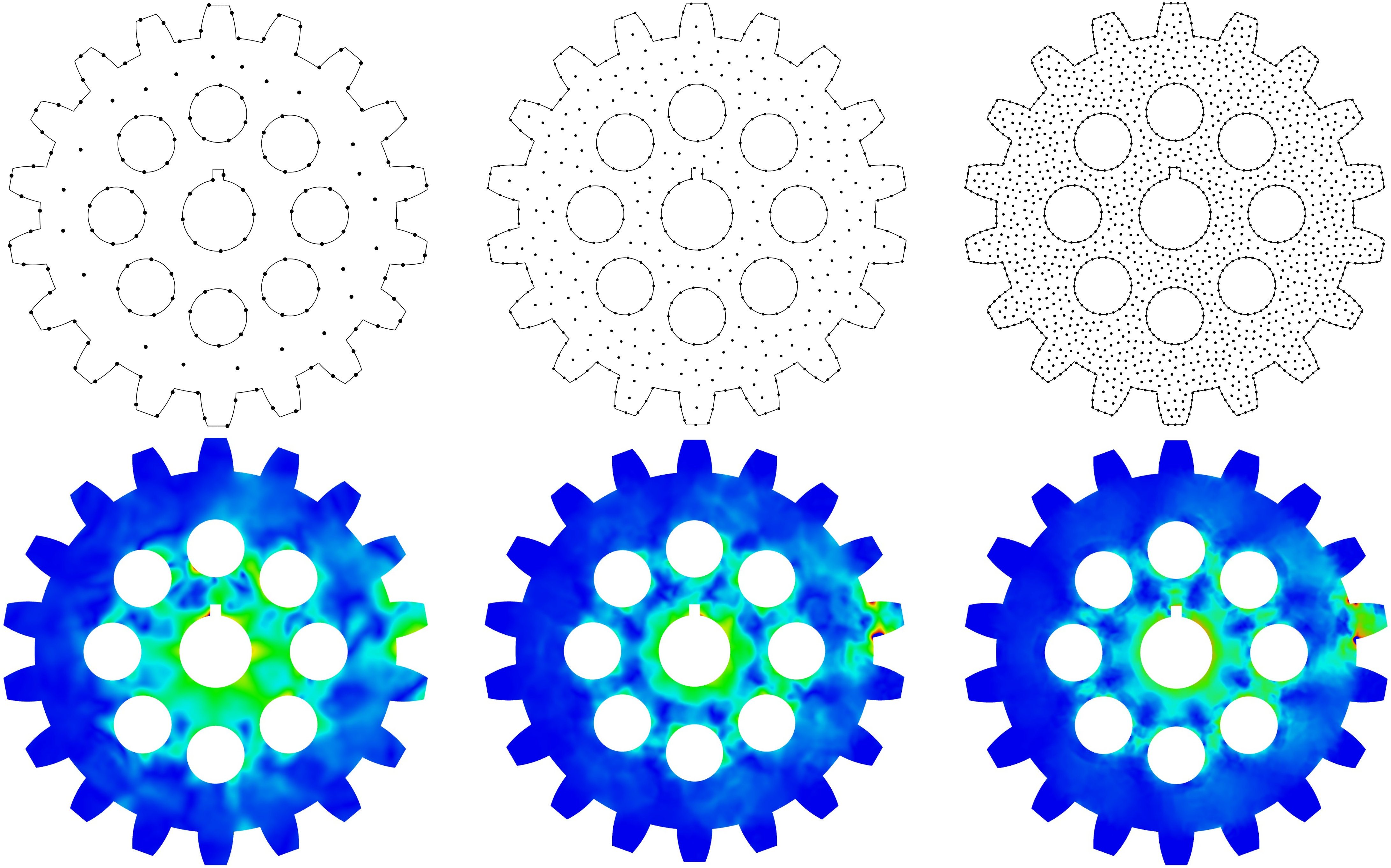

Nearly incompressible limit

- Can extend approach to handle nearly incompressible materials
- Use a “generalized” B-Bar/F-bar approach.
- Project dilatational portion of deformation gradient to smaller subspace, e.g. use original DOF points as quadrature basis.

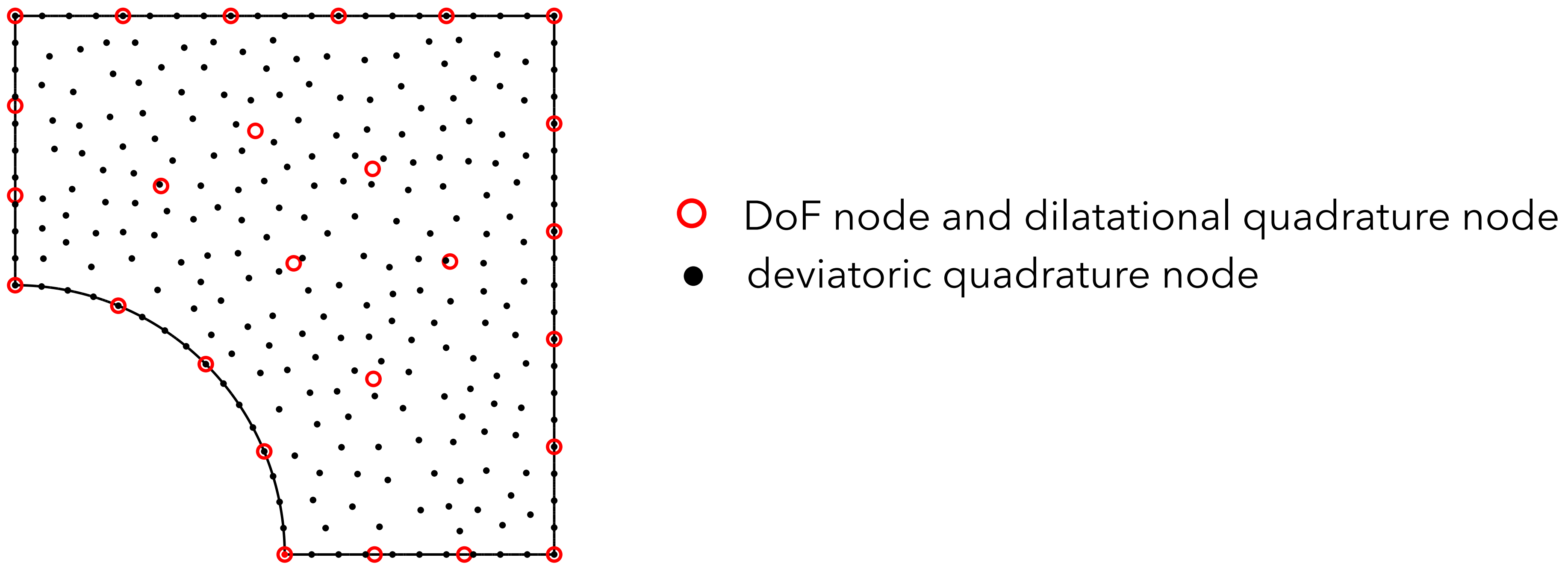

Summary

1. Separate domain discretization from solution discretization (fine-scale domain triangulation with coarse-scale solution discretization).
2. Example of discretization-based reduced order model.
3. Generation of meshfree weight functions using manifold geodesics.
4. New approach to quadrature for meshfree methods based on secondary basis.
5. Projected shape-function gradients using dual basis for polynomial consistency.
6. Observed optimal convergence rates for 2D elasticity.
7. Applicable to nonlinear solid mechanics too (plasticity).
8. Examples here were in H^1, also can be extended to H(div) and H(curl)

Coercivity

For Lax-Milgram theorem (existence and uniqueness) need coercivity of the bilinear form

There exists C such that $a(u,u) \geq C||u||^2$ for all $u \in H_0^1$

quad-to-dof ratio = 1

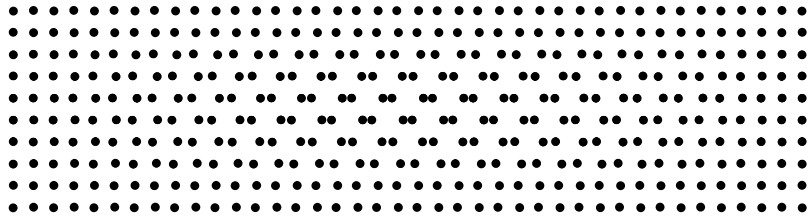

quad-to-dof ratio = 2^2

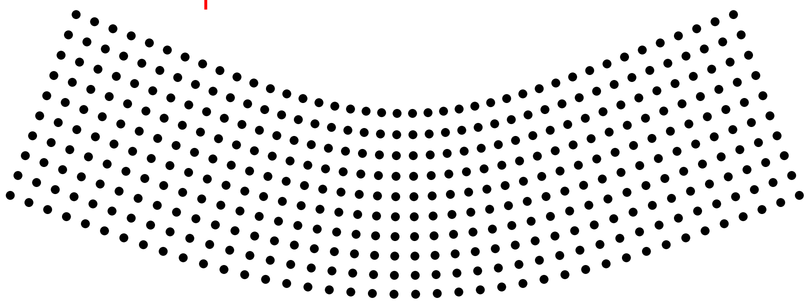

minimum eigenvalue (nonzero)